Energy &
Environmental Science

Dynamic Article Links

Cite this: *Energy Environ. Sci.*, 2011, **4**, 842

www.rsc.org/ees

PERSPECTIVE

Panchromatic engineering for dye-sensitized solar cells

Jun-Ho Yum,* Etienne Baranoff, Sophie Wenger, Md. K. Nazeeruddin and Michael Grätzel

Received 7th October 2010, Accepted 15th November 2010
DOI: 10.1039/c0ee00536c

The dye-sensitized mesoscopic solar cell has been intensively investigated as a promising photovoltaic cell. Its ecological and economical fabrication processes make it attractive and credible alternative to conventional photovoltaic systems. In contrast to the latter design, the DSC approach separates tasks of light absorption and charge transport. The primary step of light absorption is performed by a sensitizer anchored to the surface of a wide band gap semiconductor. In order to reach a high conversion efficiency, the first requirement is that the sensitizer should absorb as much as possible of the incoming sunlight. Strategies for achieving panchromatic response in dye-sensitized mesoscopic solar cells are discussed.

Introduction

The increasing global need for energy coupled with the depletion of easily accessible, hence cheap, fossil fuel reserves, poses a serious threat to the human global economy in the near future.[1,2] Considering in addition the harmful ecological impact of conventional energy sources, it becomes obvious that development of clean alternative energy sources is a necessity.[3–6] Best renewable energy options must rely on a net input of energy onto the earth. Since the sun is our only external energy source, harnessing its energy, which is clean, non-hazardous and *infinite*, satisfies the main objectives of all alternative energy strategies. Mastering the conversion of sunlight to electricity or to a non-fossil fuel like hydrogen is without any doubt the most promising solution to the energy challenge. It is remarkable that a mere 10 min of solar irradiation onto the Earth's surface is equal to the total yearly human energy consumption.

Actual commercially available photovoltaic technologies are based on inorganic materials. Their fabrication requires high costs and large amounts of energy. In addition they often use toxic and/or scarce materials. The dye-sensitized mesoscopic solar cell (dye-sensitized solar cell, DSC) avoids these pitfalls and thus represents one of the most promising methods for future large-scale power production directly from sunlight.[3,4,7–12] DSC is often included in the organic photovoltaic (OPV) family because of the organic nature of at least part of its constituents. In conventional organic photovoltaic devices, two organic materials with electron donor and acceptor character, respectively, form a heterojunction favoring the separation of the exciton formed by absorption of sunlight into two carriers. Then the same organic materials used for light absorption are used to transport the formed carriers to the electrodes. Therefore a material for classical organic photovoltaic devices should combine both good light harvesting properties and good carrier transporting properties, which is a difficult task to achieve. On the other hand, DSCs technology separates the two tasks. The dye absorbs light to form an exciton, then the charge generation is performed at the semiconductor–dye interface, and the semiconductor and the electrolyte serve as the charge transporting material.[13] Optimization of the device can therefore be done by separately modifying the dye alone to optimize the spectral properties, while carrier transport properties can be improved by optimizing the semiconductor and the electrolyte composition.

A schematic representation of the architecture of the DSC is shown in Fig. 1. The DSC architecture is broadly composed of five components: (1) a mechanical support coated with a transparent conductive oxide (TCO); (2) the semiconductor film,

Laboratory of Photonics and Interfaces, Institute of Chemical Sciences and Engineering, Ecole Polytechnique Fédérale de Lausanne (EPFL), Station 6, CH-1015 Lausanne, Switzerland. E-mail: junho.yum@epfl.ch; Fax: +41 21 693 41 11; Tel: +41 21 693 36 21

Broader context

The solar energy is clean, non-hazardous and infinite, satisfying the main objectives of all alternative energy strategies. Among various solar conversion systems, the dye-sensitized mesoscopic solar cell has been intensively investigated as a promising photovoltaic system in terms of its ecological and economical fabrication processes. One of the requirements to reach a high conversion efficiency is that the solar cell should absorb as much as possible of the incoming sunlight. This perspective review is to present the various strategies to improve the light-harvesting performance of the solar cell over the entire visible and near-IR spectrum.

Jun-Ho Yum

Dr Jun-Ho Yum *received the PhD degree in materials science and engineering from Gwangju Institute of Science and Technology (Gwangju, Republic of Korea). He worked on interfacial dynamics study of dye-sensitized solar cells in Osaka University (Osaka, Japan) and on polymer electrolyte for solar cells in Korean Institute of Science and Technology (Seoul, Korea). Since October 2005, he has worked at Ecole Polytechnique Fédérale de Lausanne (Lausanne, Switzerland). His fields of interest are dye-sensitized solar cells, nano-materials and interfaces, renewable energy and materials, energy (and hydrogen) generation and storage devices, photoelectrochemistry, and electrochemistry.*

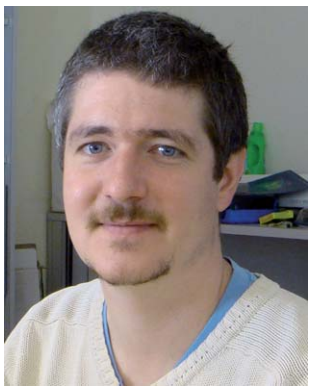

Etienne Baranoff

Dr Etienne Baranoff *completed his doctoral work about photo-induced electron transfer at the Université de Strasbourg in professor Sauvage's group. Then he worked as a JSPS post-doctoral fellow at the University of Tokyo with professor Kato to study about supramolecular liquid crystals and soft matter in general. He is currently a research associate at Ecole Polytechnique Fédérale de Lausanne (EPFL) in professor Grätzel's group where he develops new transition metal complexes for various light-related applications such as OLEDs, DSCs, and sensors.*

Sophie Wenger

Dr Sophie Wenger *recently obtained her PhD from the Ecole Polytechnique Fédérale de Lausanne (EPFL), where she conducted work on the optimization of dye-sensitized solar cells in the group of Prof. Michael Grätzel. She holds a masters degree in physics from the Eidgenössische Technische Hochschule (ETH) Zurich. Her research interests include tandem device architectures, organic sensitizers, and numerical device modeling of dye-sensitized solar cells.*

usually TiO_2; (3) a sensitizer adsorbed on the surface of the semiconductor; (4) an electrolyte containing a redox mediator; and (5) a counter electrode capable of regenerating the redox mediator. Since it is a low cost, widely available and non-toxic material, titanium dioxide has become the semiconductor of choice for the photoelectrode. The most commonly used redox mediator is the redox couple iodide/triiodide. Ruthenium complexes such as [Ru(4,4′-dicarboxylic acid 2,2′-bipyridine)$_3$][14] were employed as sensitizers very early on and are still now the most commonly used sensitizers. A very important factor for the success of the DSC is the high surface area obtained by the semiconductor film made of nanoparticles. It leads to increased dye loading when compared to single crystals, thus increasing

Mohammad. K. Nazeeruddin

Dr Mohammad. K. Nazeeruddin *is a Senior Scientist at EPFL, Switzerland, and holds a World Class University (WCU) professor appointment in the Department of Materials at the Korea University, Jochiwon, Korea. His current research focuses on dye-sensitized solar cells, light-emitting diodes and chemical sensors. He has published more than 220 peer-reviewed papers, nine book chapters, and inventor of 25 patents. He appeared in the ISI listing of most cited chemists, and has more than 12 500 citations with an* h*-index of 55.*

Michael Grätzel

Professor at the Ecole Polytechnique Fédérale de Lausanne, ***Michael Grätzel*** *pioneered research on energy and electron transfer reactions in mesoscopic-materials and their application in solar energy conversion systems* i.e. *dye-sensitized solar cells, optoelectronic devices and lithium ion batteries. Author of over 800 peer-reviewed publications, two books and inventor of more than 50 patents, his work has obtained 60 000 citations so far (*h*-index 114), ranking him amongst the 10 most highly cited chemists worldwide. He has received prestigious awards, including the 2010 Millennium Technology Prize, the City of Florence Award, the Balzan Prize, the Galvani Medal, the Faraday Medal, the Harvey Prize, the Gerischer Award, the Dutch Havinga Award and Medal, the International Prize of the Japanese Society of Coordination Chemistry, the ENI-Italgas Energy-Prize and the year 2000 European Grand Prix of Innovation. He was selected by the Scientific American as one of the 50 top researchers in the world.*

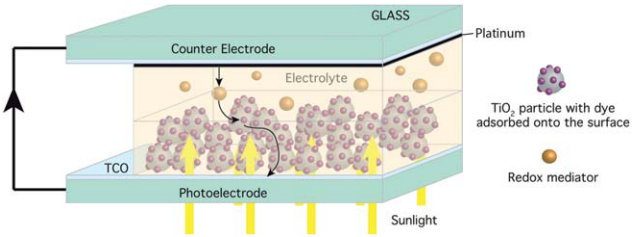

Fig. 1 Schematic representation of the dye-sensitized solar cell.

optical density and resulting in efficient light harvesting. While the total efficiency of the dye-sensitized solar cell depends on the optimization and compatibility of each of its constituents, the initial requirement is for the device to be able to gather as many photons from sunlight as possible. The scope of this perspective review is to present the various strategies to improve the light-harvesting performance of the DSC over the entire visible and near-IR spectrum.

Operating principle of DSCs

The operating principle of the DSC including an indicative energy band diagram is shown in Fig. 2. Since the scope of this perspective review is centered on panchromatic engineering, the operating principle will be briefly presented. Details can be found elsewhere.[15–18]

First, the sensitizer S is excited by absorption of a photon (eqn (1)). Then the excited sensitizer S* injects an electron into the conduction band of the semiconductor (eqn (2)). The injected electron flows through the semiconductor network to the back contact and then through the external load to the counter electrode where it reduces the redox mediator (eqn (3)), which in turn regenerates the oxidized sensitizer S^+ (eqn (4)). This completes the circuit. Under illumination, the device constitutes a regenerative and stable photovoltaic energy conversion system.

$$S_{(adsorbed)} + h\nu \rightarrow S^*_{(adsorbed)} \quad (1)$$

$$S^*_{(adsorbed)} \rightarrow S^+_{(adsorbed)} + e^-_{(injected)} \quad (2)$$

$$I_3^- + 2e^-_{(cathode)} \rightarrow 3I^-_{(cathode)} \quad (3)$$

$$S^+_{(adsorbed)} + \frac{3}{2}I^- \rightarrow S_{(adsorbed)} + \frac{1}{2}I_3^- \quad (4)$$

The overall efficiency of the device depends on optimization and compatibility of each of the constituents. Losses occur mainly through the recombination of the injected electrons either with the oxidized sensitizer (eqn (5)) or with the oxidized redox couple at the TiO_2 surface (eqn (6)).

$$S^+_{(adsorbed)} + e^-_{(TiO_2)} \rightarrow S_{(adsorbed)} \quad (5)$$

$$I_3^- + 2e^-_{(TiO_2)} \rightarrow 3I^-_{(anode)} \quad (6)$$

The incident monochromatic photon-to-current conversion efficiency (IPCE also called EQE (External Quantum Efficiency)) is related to the light-harvesting performance of sensitizer. It is defined as the number of photo-electrons in the external circuit

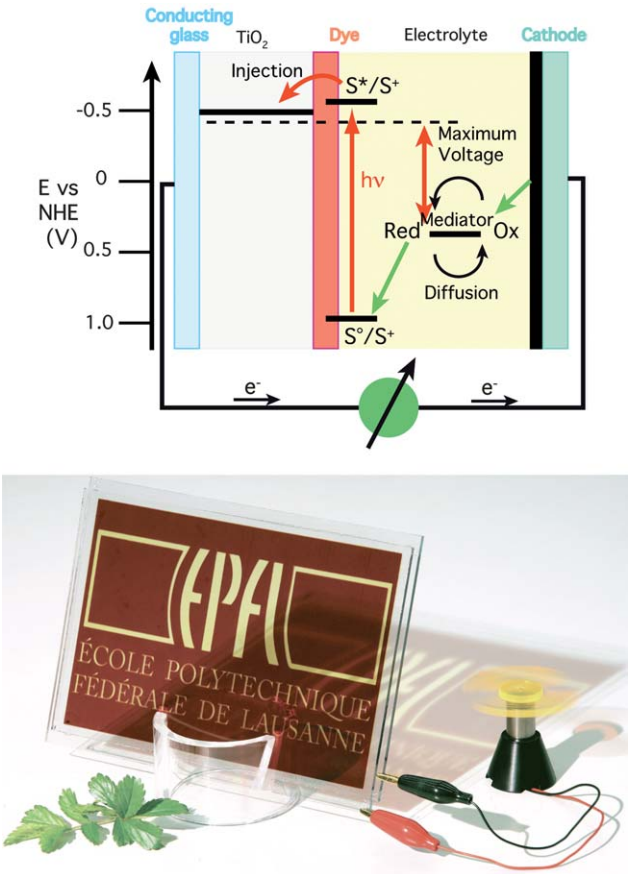

Fig. 2 (Top) Operating principles and energy level diagram of dye-sensitized solar cell. $S^\circ/S^+/S^*$ = sensitizer in the ground, oxidized and excited state, respectively. Red/Ox = Redox mediator. (Bottom) Example of a DSC (Ecole Polytechnique Fédérale de Lausanne).

divided by the number of incident photons as a function of excitation wavelength as in (eqn (7)):[19]

$$\mathrm{IPCE}(\lambda) = \frac{\text{photocurrent density}}{\text{wavelength} \times \text{photon flux}} = \mathrm{LHE}(\lambda) \times \varphi_{inj} \times \eta_{coll} \quad (7)$$

where LHE(λ) is the light-harvesting efficiency at wavelength λ, φ_{inj} is the quantum yield for electron injection from the excited sensitizer in the conduction band of the TiO_2, and η_{coll} is the efficiency for the collection of electrons.

The overall conversion efficiency (η) of the dye-sensitized solar cell is determined by the photocurrent density (J_{sc}), the open circuit potential (V_{oc}), the fill factor (ff) of the cell and the intensity of the incident light (I_0) (eqn (8)):[20]

$$\eta = \frac{J_{sc} \times V_{oc} \times \mathrm{ff}}{I_0} \quad (8)$$

It can be seen that increasing the photocurrent density will improve the conversion efficiency of the device. This is achieved by improving the light harvesting efficiency of the sensitizer system.

Ideally, all photons below a threshold wavelength of about 920 nm should be harvested and converted into electric current. This limit is derived from thermodynamic considerations showing that the conversion efficiency of any single-junction

photovoltaic solar converter peaks at approximately 33% near a threshold energy of 1.4 eV.[21,22] The other essential property required for the light-harvesting system of a molecular/semiconductor junction is that the sensitizer in the excited state possesses directionality. This directionality should be engineered to provide an efficient electron transfer from the excited dye to the TiO_2 conduction band *via* good electronic coupling between the lowest unoccupied molecular orbital (LUMO) of the sensitizer and the 3d orbital of titanium. Also, the sensitizer should have suitable anchoring groups for grafting the dye on the semiconductor surface to ascertain intimate electronic coupling between its excited state wave function and the conduction band manifold of the semiconductor.[7,14]

1. Panchromatic harvesting by single dye

The remarkable performances of the tetraprotonated complex [*cis*-(dithiocyanato)-Ru(II)-*bis*(2,2′-bipyridine-4,4′-dicarboxylate)] (N3)[23] and its doubly deprotonated analogue, complex (N719)[14] (see the molecular structure in Fig. 4(a)) had a central role in advancing significantly the DSC technology. The photovoltaic performance of N719 is superior to that of compound N3 due to a higher V_{oc} and a comparable J_{sc}. However, the main drawback of N719 is the lack of absorption in the red region of the visible spectrum.

1.1 Panchromatic Ru(II) complex. The spectral properties of ruthenium sensitizers can be tuned towards the red part of the visible spectrum by introducing a ligand with a low-lying π^* molecular orbital and by destabilization of the metal t_{2g} orbital through the introduction of a strong donor ligand (see Fig. 3). The former lowers the energy of the lowest unoccupied molecular orbital (LUMO) while the latter destabilizes the highest occupied molecular orbital (HOMO) of the sensitizer, ultimately reducing the HOMO–LUMO gap. However, the extension of the spectral response into the near-infrared region by lowering the LUMO energy is limited to LUMO energy levels from which charge injection into the TiO_2 conduction band can occur.[24–26] Likewise, near-IR response by destabilization of Ru t_{2g} (HOMO) levels close to the redox potential of the redox mediator also is unfavorable because of problems associated with regeneration of the oxidized dye following the electron injection into TiO_2. Therefore, the optimum ruthenium sensitizers should exhibit an excited state oxidation potential of at least −0.9 V *vs.* SCE

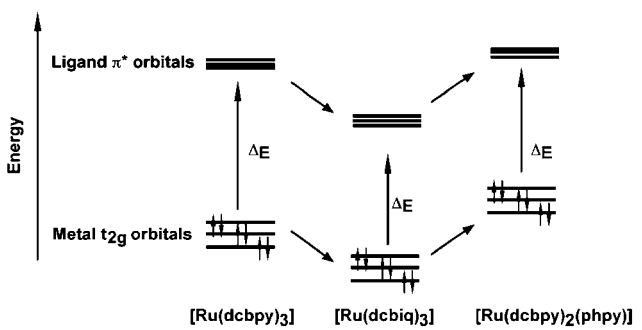

Fig. 3 Schematic representation of tuning the HOMO (t_{2g}) and LUMO (π^*) orbital energy.[27] dcbpy: 4,4′-dicarboxy-2,2′-bipyridine; dcbiq: 4,4′-dicarboxy-2,2′-biquinoline; phpy: phenylpyridine.

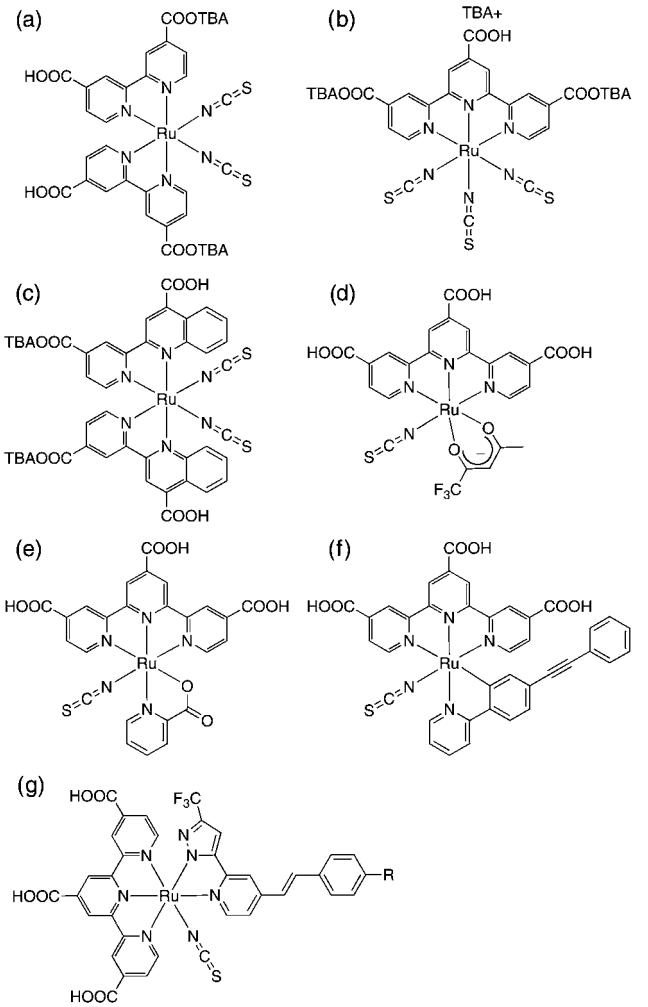

Fig. 4 Molecular structures of (a) N719, (b) N749, (c) $[NBu_4]_2$-$[Ru(Hdcpq)_2(NCS)_2]$, (d) Ru(tctpy)(tfac)(NCS), (e) Ru(tctpy)(pc)-(NCS), (f) Ru(tctpy)(C^N)(NCS), (g) Ru(tctpy)(pypz)(NCS). Hdcpq: 4-carboxy-2-[2′-(4′-carboxypyridyl)]quinoline; tctpy: 4,4′,4″-tricarboxy-2,2′:6′,2″-terpyridine; tfac: 1,1,1-trifluoropentane-2,4-dionato; pc: 2-pyridinecarboxylate; C^N: 2-(4-(2-phenylethynyl) phenyl)pyridinato.

(saturated calomel electrode), in order to inject electrons efficiently into the TiO_2 conduction band,[11] while their ground state oxidation potential should be about 0.5 V *vs.* SCE, in order to be regenerated rapidly *via* electron donation from the electrolyte (iodide/triiodide redox system or a hole conductor).

To fulfill the requirement of panchromatic ruthenium complexes, N749 ("black dye") triisothiocyanato-(2,2′:6′,6″-terpyridyl-4,4′,4″-tricarboxylato) Ru(II) tris(tetra-butylammonium) (see molecular structure in Fig. 4(b)) has been synthesized in which the ruthenium center is coordinated to a monoprotonated tricarboxyterpyridine ligand and three thiocyanate ligands.[28,29]

Fig. 5 shows the photocurrent action spectrum of a cell containing N719 and N749, where the incident photon to current conversion efficiency is plotted as a function of wavelength. It is evident that the response of the N749 extends 100 nm further into the infrared than that of N719. The photocurrent onset is close to 920 nm, *i.e.* near the optimal threshold for single junction converters. From that point, the IPCE rises gradually until at 700 nm and it reaches a plateau of over 80%. From the overlap

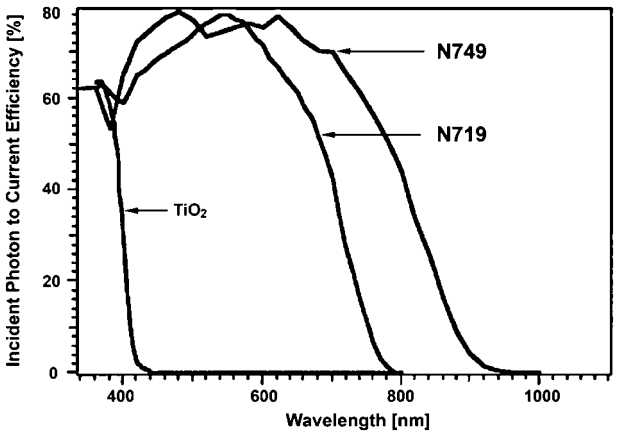

Fig. 5 IPCE obtained with the N749 attached to nanocrystalline TiO_2 films. The incident photon to current conversion efficiency is plotted as a function of the wavelength of the exciting light. IPCE for bare TiO_2 and TiO_2 sensitized with N719 have been included for comparison.

integral of the IPCE curves (Fig. 5) with the AM 1.5 solar emission, one predicts the short circuit photocurrents (J_{sc}) of N719 and N749-sensitized cells to be 16.5 and 20.5 mA cm^{-2}.[30] Routinely, the experimental photocurrents obtained with N749 are in the range of 18–21 mA cm^{-2}.[29] The open circuit potential (V_{oc}) is 720 mV, and the fill factor (ff) is 0.7, yielding for the overall solar (global AM 1.5 solar irradiance 1000 W m^{-2}) to electricity conversion efficiency (η) a value of 10.4%.[29] With the N749 dye, conversion efficiency of 11.1% has been achieved using high-haze TiO_2 electrodes by Han and colleagues.[31]

Sugihara and colleagues have shown LUMO tuning by quinoline for $Ru(dcbpy)_2(NCS)_2$ (see molecular structure in Fig. 4(c)).[25] $Ru(Hdcpq)_2(NCS)_2$ showed a 47 nm red shift at the absorption maximum with an IPCE extending beyond 900 nm. He and his team have recently extended to incorporate the quinoline moieties in terpyridyl Ru(II) complex and showed a very broad spectral response extending to ~1050 nm.[32] However, the driving force for charge injection was reduced *i.e.* 80% of N719 due to a lower LUMO, 0.24 eV below that of N719. The team has shown another type of panchromatic dye, β-diketonato tricarboxyterpyridyl Ru(II) sensitizer, with 1,1,1-trifluoropentane-2,4-dionato (tfac) in place of monodentate NCS ligands (see Ru(tctpy)(tfac)(NCS) in Fig. 4(d)).[26] Ru(tctpy)-(tfac)(NCS) exhibits an intense metal-to-ligand charge transfer (MLCT) band at 610 nm with a distinct shoulder at 720 nm. Under similar photovoltaic measuring conditions, Ru(tctpy)-(tfac)(NCS) showed higher IPCE values between 720 and 900 nm than N749. However, a low V_{oc} limited the power conversion efficiency. To overcome the drawback, Han and colleagues have synthesized substituted β-diketonato Ru(II) sensitizer, Ru(tctpy)(tffpbd)(NCS)$(TBA)_2$ (tffpbd = 4,4,4-trifluoro-1-(4-fluorophenyl)butane-1,3-dione), which yielded a conversion efficiency η of ~9.0% and photocurrent density J_{sc} of ~20.0 mA cm^{-2}.[31,33] However, the substitution of two thiocyanato ligands by a fluorine-substituted tffpbd chelating ligand stabilizes the ground state by withdrawing electron density from the ruthenium center. This stabilizes the ruthenium t_{2g} orbitals in turn blue-shifting the lowest energy MLCT band. Funaki *et al.* have shown Ru(II) tricarboxyterpyridyl with a pyridinecarboxylate ligand instead of two NCS ligands (see Ru(tctpy)(pc)(NCS) in Fig. 4(e)).[34] The lowest energy band was blue-shifted compared to that of the N719 due to the replacement of two NCS ligands with a 2-pyridinecarboxylate ligand, since the electron-donating ability of a single 2-pyridinecarboxylate ligand is inferior to that of two NCS ligands. In spite of the blue shifted MLCT peak, this sensitizer exhibits broad absorption over the visible region and a panchromatic IPCE similar to the N749 dye. Both sensitizers showed comparable DSC performance yielding in the case of Ru(tctpy)(pc)(NCS) J_{sc} of 19.8 mA cm^{-2} and η of 9.66% while J_{sc} of 19.0 mA cm^{-2} and η of 9.58% were obtained for N749. The same group has also reported a panchromatic cyclometallated Ru(II) complex, Ru(tctpy)(C^N)(NCS), where C^N is a bidentate cyclometallating ligand, 2-(4-(2-phenylethynyl) phenyl)-pyridinato (see the structure in Fig. 4(f)).[35] They observed strong π–π^* absorptions for the coordinated ligand in the UV region and broad MLCT absorption in a region of lower energy wavelengths than the UV region. The most notable feature in the absorption spectra is an absorption band above 700 nm with a distinct shoulder around 800 nm. These bands are attributed to a spin-forbidden MLCT absorption.[36] The dye showed absorption maxima at 749 nm (ε = 2700 M^{-1} cm^{-1}) and 733 nm (ε = 4000 M^{-1} cm^{-1}), respectively, due to the introduction of a C^N ligand. DSCs with the dye showed an IPCE value of 10% at 900 nm and an onset IPCE at 1000 nm. Ru(II) terpyridine bearing pyridine pyrazolate (pypz) (see molecular structure in Fig. 4(g)) has been recently reported by Chou and co-workers.[37] The substitution drastically increased the molar extinction coefficient in the wavelength range 400–550 nm even though the MLCT band at 520 is blue shifted when compared to the N749 dye. Substituting H, OMe, OC_8H_{17}, or *tert*-butyl groups onto the pypz ligand of the complex produced a very comparable J_{sc} (1.0–1.1 times as high as in device with the N749). Moreover, a long hydrophobic alkoxy chain or *tert*-butyl group resulted in ~30 mV gain in V_{oc} which led to over 10% power conversion efficiency.[37]

1.2 Panchromatic ruthenium free organic dyes. Metal-free dyes have been intensively investigated to replace Ru complexes as sensitizer for DSCs.[38,39] However, compared to Ru sensitizers, metal-free dyes show a narrower absorption properties over the whole spectral distribution of sunlight, with successful panchromatic metal-free dyes have rarely been demonstrated. Recently Sun and colleagues have reported a metal-free panchromatic dye TH304 (see molecular structure in Fig. 6) which incorporates the phenoxazine (POZ) subunit as an electron donor and co-rhodamine as the electron acceptor.[40] It is

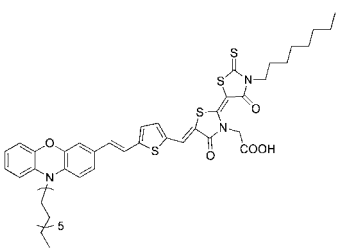

Fig. 6 Molecular structure of TH304.

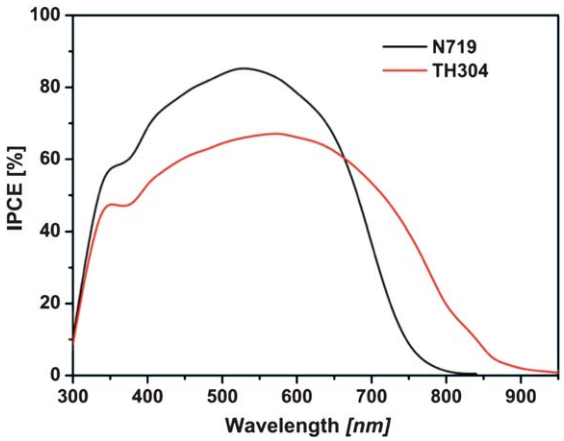

Fig. 7 The IPCE spectra of DSCs based on N719 dye (black line) and TH304 dye (red line). Taken from Fig. 4 of ref. 40.

worth noting that metal-free organic dyes are mainly composed of an electron donor (D) and acceptor (A) moiety, which are connected *via* a π-conducting bridge. Fig. 7 shows the IPCE spectrum of DSC based on and the TH304 (black line) dye. Notably, it shows a broader IPCE spectrum from 300 nm to 920 nm with a maximum value of 67% at 580 nm. However, the IPCE is not high enough to overcome N719's power conversion efficiency due to a low directionality, which is ascribed to localised electron density on the thienyl and co-rhodanine framework due to the presence of the methylene group.[41] Although the dye provides a low η of 3.0% due to the low IPCE, the discovery possibly paves the way to improving the absorption characteristics of metal-free dyes in the near-IR region.

1.3 Semiconductors. The utilization of semiconductors as light absorbing material in place of dye molecules has recently been drawing much attention. Their advantages include a high light harvesting capability,[42,43] a tuneable band gap over a wide range,[44,45] and a large intrinsic dipole moment.[46] A range of semiconductors have been investigated, including PbS,[47] CdS,[48] CdSe,[49–52] CdTe,[53] In_2S_3,[54] $Cu_{2-x}S$,[55] and $CuInS_2$.[56] Among them, PbS has a very broad light harvesting ability throughout the visible spectrum because of its small band gap (bulk energy band gap ~0.41 eV) and its large exciton Bohr radius of 20 nm leading to a high quantum efficiency.[57] The injection yield is dependent on energy level difference from conduction band of semiconductors to TiO_2 conduction band. The small energy difference attained by decreasing the particle size of CdSe on TiO_2 is sufficient to increase the electron injection rate by nearly 3 orders of magnitude.[58] Hyun *et al.* have reported the size limitation of PbS, that is 4.3 nm for the efficient charge injection to TiO_2 nanoparticles.[59] Recently, a very broad IPCE has been reported for PbS deposited by SILAR (Successive Ionic Layer Adsorption and Reaction) method with $[Co(o\text{-phen})_3]^{2+/3+}$ as redox couple.[60] The well-known and most efficient I^-/I_3^- redox couple is not compatible with low band gap semiconducting materials, leading to a rapid corrosion of the semiconductors. As can be seen in Fig. 8, the IPCE value was over 50% throughout a large part of the visible range, and its tail extended up to 900 nm or more.

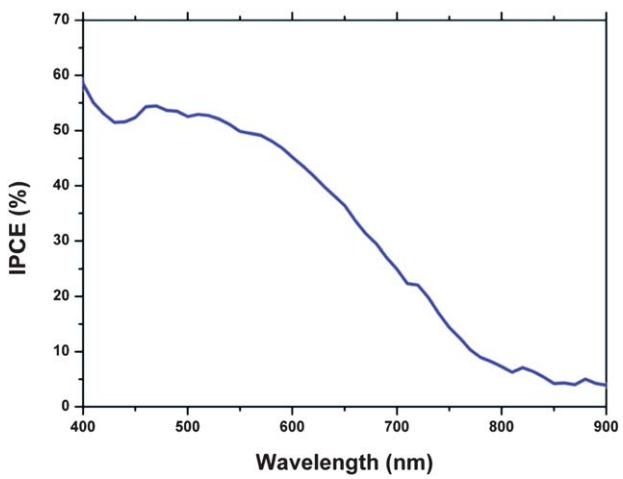

Fig. 8 The IPCE spectrum of DSCs based on PbS-sensitized cell working with a regenerative cobalt complex, $[Co(o\text{-phen})_3^{2+/3+}]$.[60]

2. Panchromatic harvesting by multiple dyes

It is a very difficult task to design a single sensitizer that absorbs efficiently over the entire visible and near IR spectrum that is from 400 to 920 nm and fulfills all the requirements necessary to obtain an efficient device performance. However, it is possible to develop efficient sensitizers that are sensitive in a smaller part of the 400–920 nm region. Therefore the combination of multiple dyes is seen as a promising approach to obtain panchromatic systems.

2.1 Co-sensitization with red light absorbing dyes. The main drawback of ruthenium-based sensitizers and organic sensitizers introduced above is the difficulty to have strong absorption in the red region of the visible spectrum. These systems can be improved simply by combination with another sensitizer absorbing mainly in the red to near-IR part of the spectrum. Mixtures of two sensitizers having complementary absorption properties and both being able to attach to the TiO_2 surface are used as "dyes cocktails" for co-sensitization to achieve panchromatic sensitization. Zhang and colleagues have shown that squarylium cyanine dye in cocktail with N3 dye improved the efficiency by 12% relative to that of single N3 by extending the absorption range into the red.[61] In another example, Spitler and colleagues have used di-carboxylated cyanine dyes and shown the photocurrent from a mixture of three dyes covering altogether most of the visible light region.[62]

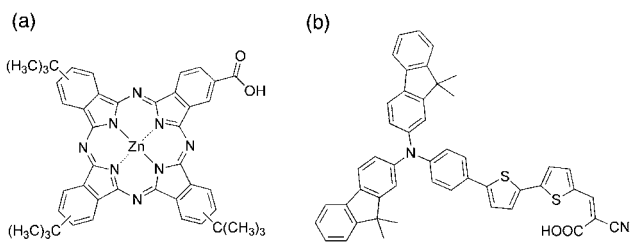

Fig. 9 Molecular structures of (a) TT1 and (b) JK2.

In order to maximize the co-sensitization effect, one of the most important prerequisites is the LHE of individual dyes. Indeed, the overall amount of dye attached to the titania surface is limited. Hence, in order to maximize the LHE, sensitizers having intense absorption in the near-IR regions should be considered for this architecture. In this respect, phthalocyanines (Pcs) will be discussed because they meet most of the requirements of an efficient sensitizer in the far red region though they have no response in the visible light region. They are therefore particularly relevant for co-sensitization with sensitizers having good spectral response in the visible region only.

Phthalocyanines (Pcs) exhibit absorption maxima at around 700 nm with very high extinction coefficients (where the maximum of the solar photon flux occurs) that make them especially suitable for integration in light energy conversion systems.[63] TT1 (Fig. 9(a) for molecular structure) has been reported as one of the successful Pcs for application in DSCs.[64] In the TT1, three *tert*-butyl groups and one carboxylic acid group act to "*push*" and "*pull*", respectively. The function of the carboxylic acid group is to graft the sensitizer on the semiconductor surface and to provide intimate electronic coupling between its excited state wave-function and the conduction band manifold of the semiconductor. The purpose of the three *tert*-butyl groups is to enhance the solubility, to minimize aggregation, and to tune the LUMO level of the Pc that provides directionality in the excited state.[64] The IPCE of TT1 itself reached 80% and a second organic dye, JK2 (3-{5′-[*N*,*N*-bis(9,9-dimethylfluorene-2-yl)phenyl]-2,2′-bithiophene-5-yl}-2-cyanoacrylic acid, see Fig. 9(b))[65] was introduced to match the optical window of TT1. Fig. 10 shows the IPCE spectrum of the co-sensitized DSC and the photoresponse of the cell extends up to 700 nm with an IPCE value of 72% at 690 nm, which corresponds to the Q band of TT1. The overall device efficiency one day after the preparation of the device was 7.74% due to a dramatic increase in J_{sc} of 16.20 mA cm^{-2} when compared to single TT1 cell yielding J_{sc} of 7.6 mA cm^{-2} and η of 3.53%.

In most of co-sensitization studies, the limited number of sites on the TiO_2 surface to which dye molecules attach places a constraint on the light absorption. Recently, a combination of black dye with organic dye (see Fig. 11) has successfully achieved

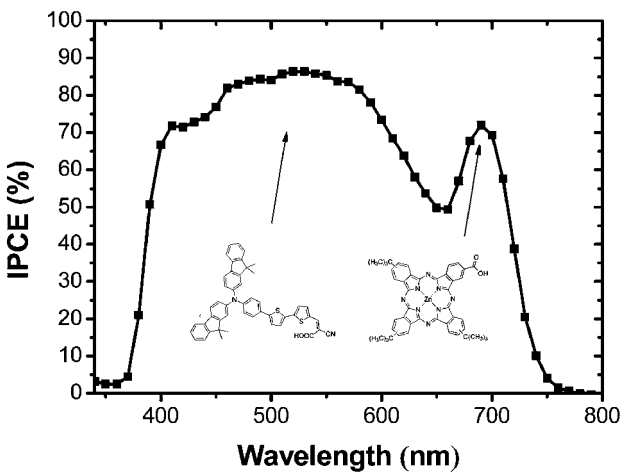

Fig. 10 The IPCE spectrum of co-sensitized DSC.

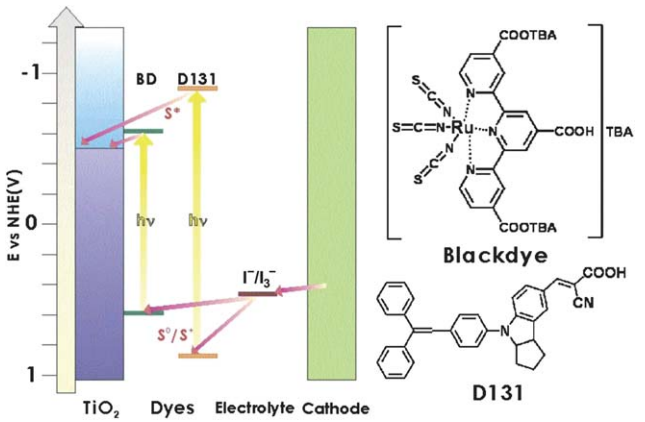

Fig. 11 Schematic of operation of the dye-sensitized solar cell with the multiple dye system using black dye and D131. Black dye is denoted as BD. Taken from Fig. 1 of ref. 66.

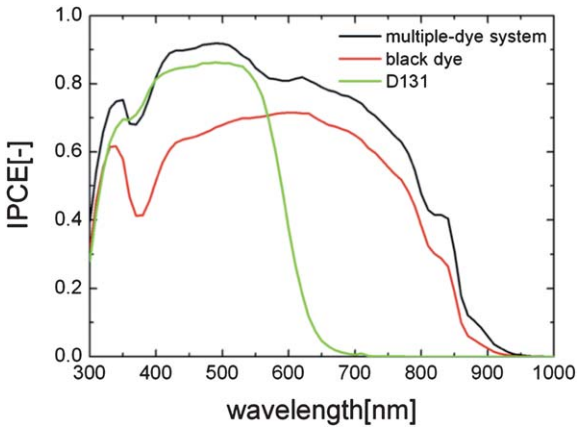

Fig. 12 IPCEs for black, D131, and co-sensitizer in the DSC. Taken from Fig. 1 of ref. 66.

11.0%, as reported by a Sony research team.[66] They presented an interesting result that no competition of dye adsorption was found due to different adsorption sites for both dyes. Moreover, D131 organic dyes improved the black dye dispersion on TiO_2, acting as a co-adsorbent.[67] Therefore, the IPCE of the co-sensitized cell surpassed that of the respective black and D131 dyes over the whole visible range (see Fig. 12).

2.2 Layered co-sensitization. Co-sensitization of titania by dyes with complementary absorption spectra has been demonstrated above. However, the limited number of sites on the TiO_2 surface to which dye molecules attach places a constraint on the light absorption achievable by co-sensitization (except with N749 dye). In fact, the magnitude of the IPCEs of co-sensitized solar cells has been shown to slightly decrease compared to the IPCEs of single cells.[64,68] Furthermore, unfavorable interactions between two or three dye molecules often decrease photovoltaic performances. Hayase and colleagues have realized a dye-bilayered structure.[69] They were inspired by fast molecular diffusion in a supercritical CO_2 condition[70] and made a swift uptake of N3 and N749 (black) dye on the TiO_2 surface.[71] Fig. 13 shows the preparation procedure of the dye-bilayer for dye adsorption.

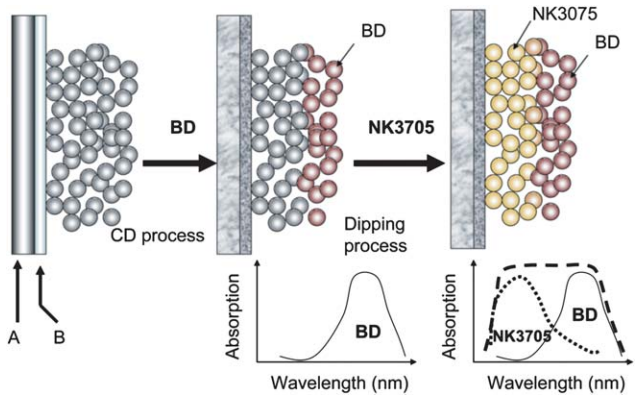

Fig. 13 Fabrication process of dye-bilayer on TiO_2 and image of light-harvesting as dye uptake. A: glass, B: F doped SnO_2, BD: black dye, and CD process: pressurized CO_2 condition. Taken from Fig. 1 of ref. 69.

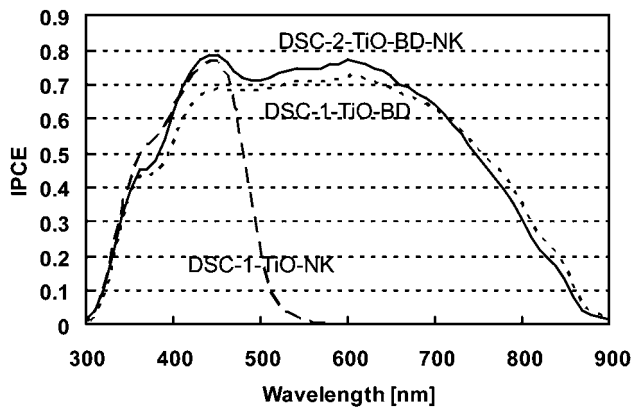

Fig. 14 IPCEs of dye-bilayer and single layer on TiO_2. Taken from Fig. 3 of ref. 69.

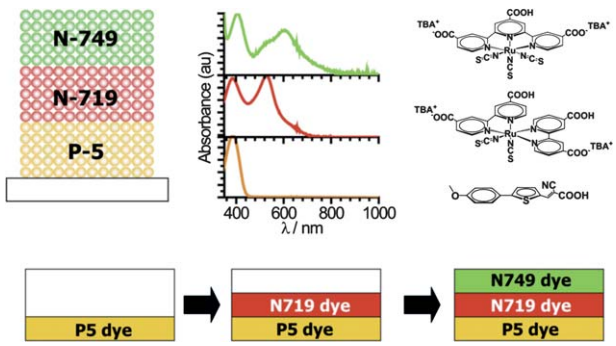

Fig. 15 Selective positioning of three dyes and their corresponding absorption spectra and molecular structures. Taken from Fig. 5(a) of ref. 72.

The black dye adsorption was controlled to be consecutively done from the top of the TiO_2 under pressurized CO_2 condition and the rest of the unstained TiO_2 surface was covered by a second dye, NK3705 (3-carboxymethyl-5-(3-(4-sulfobutyl)-2(3H)-bezothiazolylidene)-2-thioxo-4-thiazolidinone, sodium salt, Hayashibara, Co. Ltd.). The bilayer structure resulted in a J_{sc} of 21.8 mA cm^{-2} and a broad IPCE without losses in maxima as shown in Fig. 14.

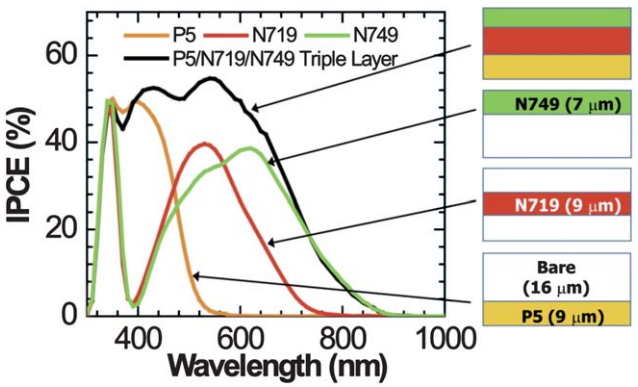

Fig. 16 IPCE of triple layer (black line) and those of the single dye, P5 (yellow line), N719 (red line), and N749 (green line). Taken from Fig. 5(c) of ref. 72.

Park and colleagues have explored a dye deposition method on the desired site in a TiO_2 film based on the column chromatographic principle.[72] The principle is that the mobile phase passes slowly through the stationary phase with a retention time and the slow flow rate of the mobile phase can help us separate each compound. They explored the selective desorption process by controlling the pore size of the TiO_2 film and the desorption rate. In brief, they polymerized a styrene oligomer in the TiO_2 mesoporous film after a normal sensitization process and then desorbed the dye in a NaOH solution with polypropylene glycol (PPG). The polystyrene coating reduced the pore size and the PPG controlled the penetration rate of the Na^+ and OH^- ions. In consequence, the dye on the TiO_2 film was able to be selectively desorbed from the top of the film, and the following dye covered on the selectively desorbed region. The repeated desorption and adsorption process allowed a selective positioning of P5 (2-cyano-3-(5-(4-ethoxyphenyl)thiophen-2-yl)acrylic acid), N719 and N749 dyes as shown in Fig. 15. Fig. 16 shows the IPCE of devices with single dyes and of the resulting three-dye cell, and demonstrates that the proposed method is promising to use of the full spectrum in DSCs.

3. Energy down conversion by energy relay dye

We discussed co-sensitization of titania by dyes with complementary absorption spectra to enhance light absorption and broaden the spectral response of organic DSCs. However, the limited number of sites on the titania surface to attach dye molecules places a constraint on the light absorption achievable by co-sensitization. Furthermore, co-sensitization requires that each dye adsorbs strongly on the surface, transfers charge efficiently into the TiO_2,[23,73–75] has slow recombination kinetics (*i.e.* in the millisecond time domain),[74,76–78] and be regenerated by the redox couple.[79] A recent study has demonstrated the use of Förster resonance energy transfer between covalently linked energy donor molecules and the sensitizing dye attached on the TiO_2 surface.[74] Siegers and colleagues were able to demonstrate a high excitation transfer efficiency (>85%) between attached dye molecules and an improvement in the device external quantum efficiency of 5–10% between 400 and 500 nm. However, the overall power conversion efficiency enhancement of the DSC was

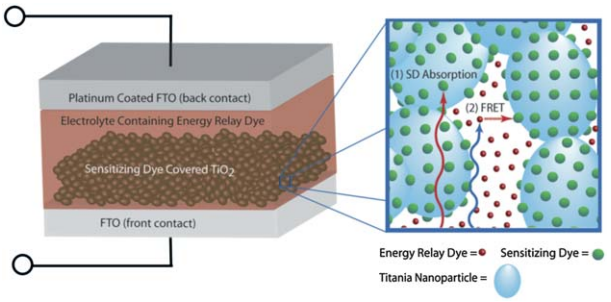

Fig. 17 Schematic representation of a DSC with energy relay dyes (ERDs). The right side of the figure shows the typical absorption process for lower energy (red) photons in the DSC: light is absorbed by the sensitizing dye (1), transferring an electron into the TiO_2, and a hole is transported to the back contact through the electrolyte. The ERD process is similar, except that higher energy (blue) photons are first absorbed by the ERD, which undergoes Förster energy transfer (2) to the sensitizing dye (SD).[82]

low (<9%) and linked more to an increase in the V_{oc} rather than to an increase in the J_{sc}.[80,81]

We recently demonstrated a new DSC architecture where highly luminescent energy relay dyes (ERDs) dissolved inside the electrolyte absorb higher energy photons and transfer their energy to the sensitizing dye *via* Förster resonance energy transfer (FRET).[82–84] Fig. 17 shows two routes for charge generation incorporated in this system. One is the typical sensitizing process, an electron into the TiO_2 and a hole into the electrolyte from the sensitizing dye (SD) (1). Second is excitation of the unattached energy relay dye (ERD) by higher energy photons which then undergoes FRET (2) to the SD. This design is analogous to photosynthesis in purple bacteria, where an aggregate of light-harvesting pigments transfers their energy to the reaction centre, initiating charge separation.[85] In particular, the pigment LH-II is not in direct contact with the reaction centre, and transfers its excitation by means of an intermediate pigment (LH-I) in under 100 ps with ~95% efficiency.[86,87] FRET involves dipole–dipole coupling of two chromophores, known as the donor and acceptor, through an electric field.[88] An excitation of the donor, or in our case the ERD, can be transferred non-radiatively through the field to the acceptor, or SD, if there is overlap between the emission spectrum of the donor and the absorption spectrum of the acceptor. Efficient energy transfer over 3–8 nm can be achieved with a strong spectral overlap and high donor emission efficiencies, for an isotropic alignment between individual chromophores in solution. If, however, the single acceptor chromophore is replaced by a dense two-dimensional array (that is, SDs tightly packed on the titania surface) FRET can become efficient well over 25 nm from the interface.[89]

As an application to the real DSC device, we demonstrated a system based on SQ1 as sensitizer combined with N877, a phosphorescent ruthenium complex, as the unattached ERD in devices with liquid[84] and solid[83] electrolyte (see molecular structures of dyes in Fig. 18). The SQ1 solution in ethanol shows absorption maxima at 636 nm with a high molar extinction coefficient ($\varepsilon = 158\ 500\ M^{-1}\ cm^{-1}$).[90] The absorption matches the emission of N877 (broad emission with a maximum at 612 nm).[91] On the other hand, N877 shows a broad absorption between 400 and 500 nm, with a maximum at 460 nm of 33 000 $M^{-1}\ cm^{-1}$,

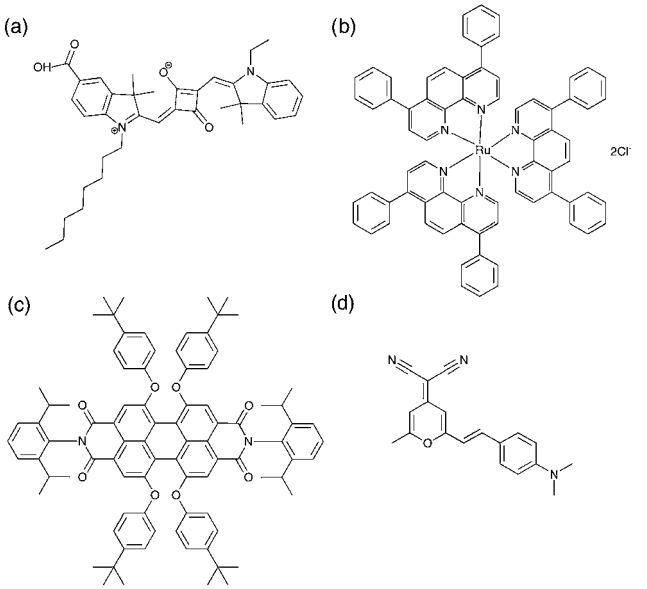

Fig. 18 Molecular structures of (a) SQ1, (b) N877, (c) PTCDI and (d) DCM.

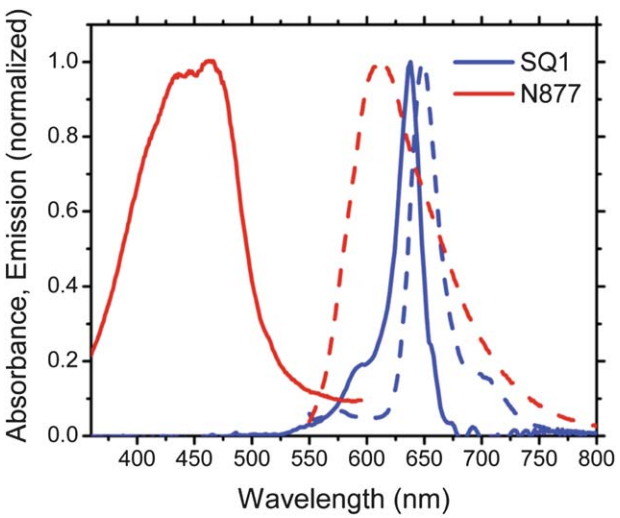

Fig. 19 Normalized UV/vis absorption (solid line)/emission (dash line) spectra of SQ1 (blue) and N877 (red) in ethanol, respectively.[83]

where SQ1 does not absorb (see Fig. 19). Fig. 20 shows the emission spectra of SQ1 (10^{-6} M EtOH solution), of N877 (10^{-5} M EtOH solution), and of a mixture in ethanol containing SQ1 and N877 at 10^{-6} M and 10^{-5} M respectively. The calculated sum of the SQ1 and of the N877 emission spectra does not match the emission observed from the mixture of SQ1 and N877. In particular, the peak corresponding to the squaraine emission maximum is more intense. In addition, when the excitation spectrum is measured while following this emission maximum (648 nm), no signal corresponding to N877 is observed indicating efficient FRET. The FRET radius R_0 is defined as the distance at which the probability of FRET between donor (*i.e.*, N877) and acceptor (*i.e.*, SQ1) is 50%. The R_0 value is dependent on the photoluminescence (PL) efficiency of the ERD and the overlap

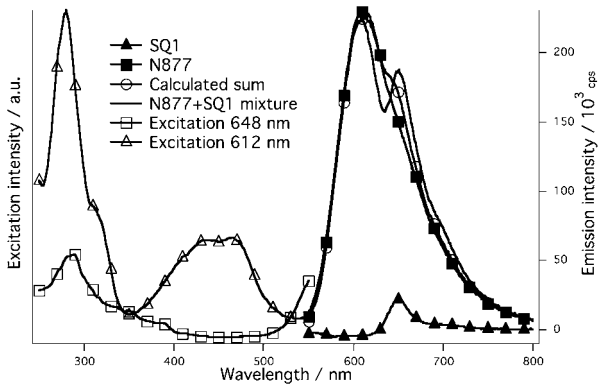

Fig. 20 SQ1 (10^{-6} M in EtOH, $\lambda_{ex} = 450$ nm), N877 (10^{-5} M in EtOH, $\lambda_{ex} = 450$ nm), calculated sum, and mixture SQ1 + N877 (10^{-6} M and 10^{-5} M respectively in EtOH) emission spectra. Taken from Fig. 2 of ref. 84.

between ERD emission (phosphorescence) and the molar extinction coefficient of the sensitizing dye. The calculated R_0 is estimated to be 5.7 nm in the range of efficient energy transfer. However, the PL of N877 is quenched by the redox media in devices, *i.e.* 69 times lower in Spiro-OMeTAD,[83] >3000 times in I^-/I_3^- system.[84] Triiodide and iodide are highly mobile ions that have a near unity probability of quenching the excited state when they collide with a chromophore.[92] Therefore FRET must occur at the subnano-second time scale in the high ionic concentrations of real devices. Hence, ERDs with a short PL lifetime (<10 ns) are required. Despite serious quenching of the N877 emission, the system SQ1/N877 leads to improved device efficiency due to an increase of blue photon harvesting. Upon adding N877, a new IPCE peak proving new electron injection by photons was generated at 470 nm, which is consistent with the absorption peak of N877 (see Fig. 21). The J_{sc} is increased by 6.7% and 30% in liquid and solid electrolyte, respectively (see Table 1). The average excitation transfer efficiency (ETE) of the ERD is given by the ratio of the internal quantum efficiency of the ERD and

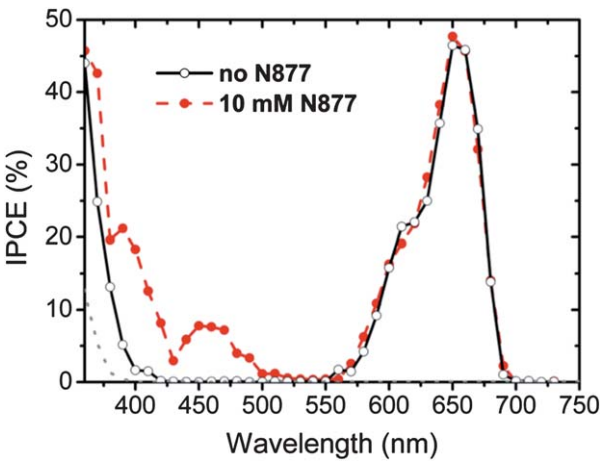

Fig. 21 IPCE spectrum of SQ1 solid-state DSCs with and without ERD, N877. The gray line is an IPCE spectrum of only Spiro-OMeTAD and the N877 energy transfer relay. The black line with open circle is only SQ1 and Spiro-OMeTAD. The red line with closed circle is SQ1 + N877 + Spiro-MeOTAD.[83]

the device.[82] The external quantum efficiency (EQE = IPCE) of the ERD is equivalent to of the product of the light harvesting efficiency and the internal quantum efficiency of the dye (eqn (9)).

$$\mathrm{ETE} = \frac{\mathrm{IQE_{ERD}}}{\mathrm{IQE}} = \frac{\mathrm{EQE_{ERD}}}{\mathrm{IQE} \times \mathrm{LHE_{ERD}}} \quad (9)$$

Another system with a derivative of perylenetetracarboxylic diimide (PTCDI, see the molecular structure in Fig. 18)[93] as ERD has been studied because PTCDI has an extremely high PL efficiency (>90%), fast fluorescence lifetime (4.8 ns, this value is three orders of magnitude faster than N877), excellent photo- and air stability and a relatively strong absorption coefficient (50 000 M^{-1} cm^{-1} at 580 nm).[94] The R_0 = 7.5–7.6 nm was determined by time-resolved PL measurements on solutions with varying concentration of TT1. The quenching rate was estimated to be ~30 times higher in real device conditions, which is much lower than in the SQ/N877 system. Devices with 13 mM PTCDI had a η of 3.21%, which is 26% higher than in a device without ERD due to an increase in the IPCE from 400 to 600 nm. A minimum ETE of 47% was calculated. It is now noted that a short lifetime of an excited state for a highly fluorescent perylene derivative is important to minimize the luminescence quenching.

Recently, an extremely high ETE of over 95% with a commercially available laser dye 4-(dicyanomethylene)-2-methyl-6-(4-dimethylaminostyryl)-4*H*-pyran (DCM) (see molecular structure in Fig. 18)[95] combined with TT1 has been reported.[96] DCM exhibits a broad absorption spectrum with a peak molar extinction coefficient of 44 900M^{-1} cm^{-1} at 460 nm and an emission overlapping with the TT1 absorption, as shown in Fig. 22. The overall dynamic quenching rate of DCM is between 5 (5 mM DCM) and 8 (22 mM DCM) times faster than the natural decay rate as observed in a practical electrolyte for the device. This is probably due to a fast PL lifetime of 1.2–2.1 ns. The R_0 from DCM to TT1 is 6.85 nm.[96] This system generated additional IPCE peaks between 400 and 550 nm, which are attributed to FRET from DCM to TT1. Fig. 23 shows ΔIPCE of 14.7%, 22.9%, and 28.2% as a function of varying DCM concentrations. The increased IPCE values indicate an ETE of >95%, which is an impressively high value.[96] Grimes and his team have reported the efficient FRET from DCM to SQ1 in the Spiro-OMeTAD system where an ETE of 67.5% was observed.[97]

4. Tandem cells

The power conversion efficiency of solar cells can be extended beyond the Shockley–Queisser limit of about 30% for a single-junction device[98] by using multiple subcells in a tandem device. Ideally, the subcells are connected optically and electrically in a series and stacked in the order of decreasing band gap, where the cell with the largest band gap is the top absorber (Fig. 24). In this way, the absorption onset of the complete device is shifted to longer wavelengths. In addition, high energy photons are converted more efficiently since thermalization losses of the generated electron-hole pairs are reduced with the graded band gap structure. In a series-connected double-junction device the ideal optical band gaps are around 1.6–1.7 eV for the top cell and 1.0–1.1 eV for the bottom cell, which extends the efficiency limit to about 45%.[99] Theoretically, the photovoltaic conversion

Table 1 Photovoltaic parameters of various SD/ERD systems measured under simulated AM 1.5G irradiance (100 mW cm^{-2})

Dye combination	J_{sc}/mA cm^{-2}	V_{oc}/mV	ff	η (%)	ETE (%)	Ref.
SQ1 (solid)	2.98	807	0.58	1.40	—	83[a]
SQ1 + N877 (solid)	3.87	786	0.59	1.80	32	
Change (%)	30	−2.7	1.7	29		
SQ1	7.48	639	0.73	3.51	—	84[b]
SQ1 + N877	7.98	638	0.72	3.67	14	
Change (%)	6.7	−0.1	−0.1	4.6		
TT1	6.88	562	0.65	2.55	—	82[c]
TT1 + PTCDI	8.78	553	0.66	3.21	47	
Change (%)	28	−1.6	−1.5	26		
TT1	8.32	582	0.72	3.50	—	96[d]
TT1 + DCM	10.61	590	0.72	4.51	95	
Change (%)	28	1.4	0	29		

[a] *Electrolyte/ERD concentration*: Spiro-OMeTAD with *tert*-butylpyridine (TBP) and $Li[CF_3SO_2]_2N$/10 mM. [b] *Electrolyte/ERD concentration:* 0.6 M 1-butyl-3-methyl imidiazolium iodide (BMII), 0.1 M LiI, 0.05 M I_2, and 0.5 M TBP in a 15/85 (v/v) mixture of valeronitrile and acetonitrile/30 mM. [c] *Electrolyte/ERD concentration*: 0.6 M PMII, ~0.01 M LiI, 0.05 M I_2, ~0.04 M TBP and ~0.02 M guanidinium thiocyanate GuNCS in chloroform/13 mM. [d] *Electrolyte/ERD concentration*: 0.6 M BMII, 0.025 M LiI, 0.04 M I_2, 0.28 M TBP, and 0.05 M GuNCS in a 15/85 (v/v) mixture of valeronitrile and acetonitrile/22 mM.

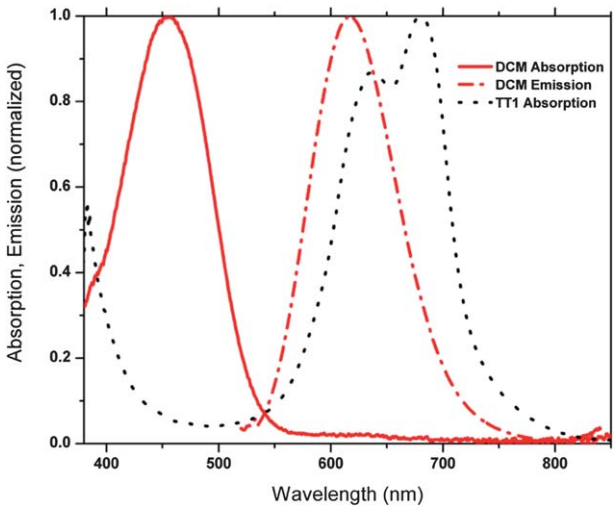

Fig. 22 Absorption (red solid line) and emission (red dash-dotted line) spectra of DCM ERD in acetonitrile : valeronitrile (85 : 15 vol) and absorption of TT1 on TiO_2 (black dotted line).[96]

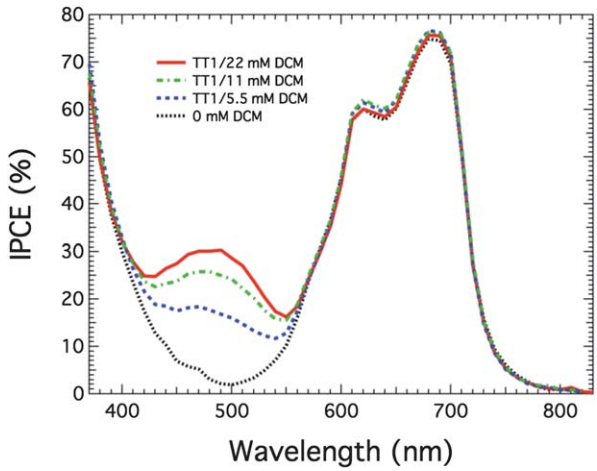

Fig. 23 IPCE of DSC based on transparent TiO_2 electrodes with varying DCM concentrations.[96]

efficiency of a tandem cell approaches the thermodynamic limit of about 85% if an infinite number of subcells and maximum solar concentration is used.[100,101] Tandem cells composed of DSCs have been studied to obtain complementary spectral response *i.e.* two photo-anode placed face-to-face,[102] or rod-type without transparent conducting glass,[103] or series-connected tandem over 10% of a conversion efficiency.[104] In this section, we present tandem configurations, DSC with chalcopyrite Cu(In,-Ga)Se_2 (CIGS) solar cell and with p-type DSC.

4.1 DSC/Cu(In,Ga)Se_2 tandem solar cells. The absorption characteristics of the dye-sensitized solar cell (DSC) and the chalcopyrite Cu(In,Ga)Se_2 (CIGS) solar cell closely match the ideal optical gap requirements for a double-junction tandem device.[99] High-efficiency DSCs use ruthenium bipyridyl complexes with an estimated excitation transition energy of $E_{0-0} \approx 1.6$–1.8 eV to convert a large fraction of the visible spectrum.[105–108] CIGS is a polycrystalline material with a direct band gap and hence a high absorption coefficient allowing for thin absorbing films (1–2 μm). The band gap of the CIGS ($CuIn_{1-x}Ga_xSe_2$) absorber can be tuned between 1.0 eV and 1.7 eV by increasing the Ga content x ($x = 0$, $CuInSe_2$ or CIS; $x = 1$, $CuGaSe_2$ or CGS). With increasing band gap, the photovoltage in a device increases, and the photocurrent decreases. Highest efficiencies are obtained with an optimized Ga content of $x \approx 0.25$ and a band gap of about 1.2 eV.[109,110] A wide range of the solar spectrum can thus be harvested in a DSC/CIGS tandem device by efficiently converting high energy photons in a top DSC and transmitted low energy photons in an underlying CIGS cell. This principle was first demonstrated with a *mechanically* stacked DSC/CIGS tandem connected in series in 2006.[111] In 2009, we reported *monolithic* integration of the two systems to cut optical losses at needless interfaces and material consumption.[112] The photovoltaic parameters for these two device architectures are shown in Table 2.

In terms of assembly, the simplest tandem structure is obtained by mechanically stacking two individual cells on top of each other (Fig. 25, left). The stacked DSC/CIGS tandem was

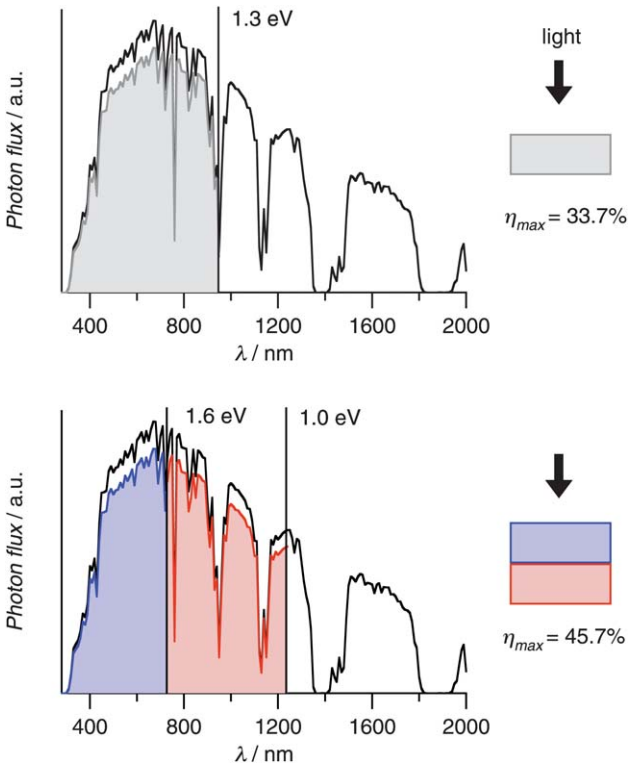

Fig. 24 Calculated ideal band gaps and maximum conversion efficiency for a single solar cell or a series-connected double-junction cell under AM 1.5G irradiance.[99] Colored areas represent the number of photons converted to electrons by the individual subcells assuming a constant external quantum efficiency of 0.9.

Table 2 Photovoltaic parameters of state-of-the-art DSC/CIGS tandem cells measured under simulated AM 1.5G irradiance (100 mW cm^{-2})

Device	V_{oc}/V	J_{sc}/mA cm^{-2}	ff	η (%)	Ref.
DSC/CIGS (stacked)	1.45	−14.1	0.74	15.1	111
DSC/CIGS (monolithic)	1.22	−13.9	0.72	12.1	112

assembled by directly stacking a DSC on a CIGS cell covered with an evaporated Al/Ni current collector grid.[111] An "index-matching" fluid (refractive index of $n = 1.7$) was used between the two cells to reduce reflection losses at the interface. This stack demonstrated the possibility of combining DSCs with CIGS thin film cells, but the obvious drawbacks of the stacked setup are reflection losses at the stack interface and absorption losses of low energy photons in the conducting glass of the top cell. In addition, the establishment of the electrical connection with the Al/Ni grid and handling of the index-matching liquid is cumbersome.

In the monolithic approach (Fig. 25, right), the top cell is directly grown or deposited on the bottom cell, leaving only two electrical contacts.[112] A monolithic assembly is clearly more advantageous, since optical losses from the superfluous layers and interfaces and material and manufacturing costs are reduced. Furthermore, all advanced tandem technologies—*e.g.* devices based on III–V semiconductors, a-Si/μc-Si, or organic semiconductors—use a monolithic assembly approach.[113–115]

As seen from IPCE measurements (Fig. 26), the DSC and CIGS show ideal onsets for use in a double-junction tandem device; the DSC converts light in the visible region with an onset at about 1.6 eV, and the CIGS converts the remaining low energy photons in the range of about 1.1–1.6 eV. Since both the stacked and the monolithic DSC/CIGS tandem devices are electrically connected in series, matching of the current densities in the subcells is crucial to minimize electrical losses. The tandem test devices generated current densities that were in the expected range for a "transparent" DSC with a 20 nm TiO_2 particle layer only (no 400 nm particle scattering layer). The measured photovoltage was close to the sum of the voltages of the individual cells, which manifests the series-connection and the reduction of thermalization losses (Table 2). So far, the monolithic integration suffers from an unfortunate drawback; the performance of the device degrades within hours. This is due to a rapid dissolution of the CdS/CIGS junction by the iodine-based electrolyte percolating through pinholes in the conducting oxide window layer (ZnO : Al or ITO) of the CIGS cell.[116] The corroding effect also explains the lower overall photovoltage obtained with the

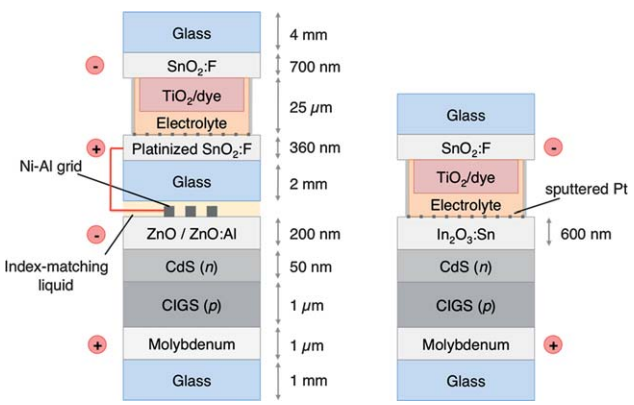

Fig. 25 Schematic of the mechanically stacked (left) and monolithic (right) tandem device structure with a DSC top absorber and a CIGS bottom absorber.

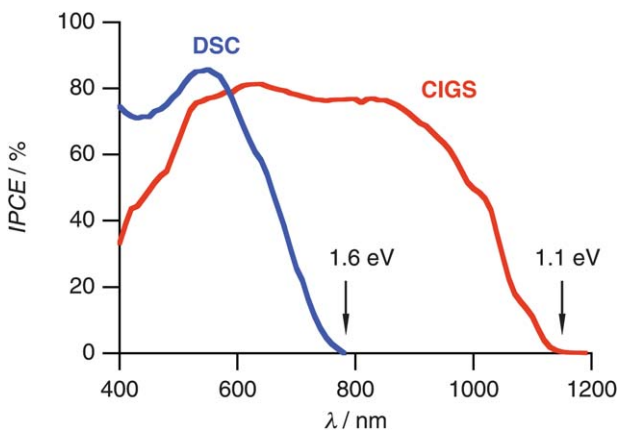

Fig. 26 IPCE of the individual DSC and CIGS cells shows ideal onsets for use in a double-junction tandem device (DSC: 8 μm TiO_2 film sensitized with C101 dye).

monolithic device. However, preliminary tests with thin protective oxide layers grown on the CIGS cell with an Atomic Layer Deposition system show a promising enhancement in stability.[117]

In the future, the optical advantages of the monolithic system should be exploitable with a suitable protective intermediate layer. Numerical simulations of the optics in the stack have shown that a balanced light absorption in the two photoactive layers (dye-sensitized TiO_2 and CIGS), yielding a photocurrent of about 16 mA cm^{-2}, can be obtained with optimized film thicknesses.[117] This is an important condition to surpass the 15.1% efficiency benchmark, given by the stacked device, with a monolithic assembly.

4.2 p-Type semiconductor. Most of the research on DSCs has been devoted to architectures based on n-type semiconductors. It is however possible to use a p-type semiconductor as photocathode. The working principle is very similar to an n-type DSC, the difference being that the excited state of the sensitizer is now reductively quenched by the semiconductor that is the sensitizer excited state injects holes into the valence band of the p-type semiconductor. The first self-operating device based on this design has been reported in 1999.[118] Odobel and co-workers have recently nicely reviewed this type of device.[119]

The development of p-type DSCs is particularly promising in view of constructing a tandem DSC. In a tandem DSC, the cathode of conventional n-type DSC is replaced by a photocathode based on a p-type semiconductor, for example based on nickel oxide (NiO). The architecture (Fig. 27) is reminiscent of the monolithic tandem device as seen in Fig. 25.

The first promising advantage of the tandem DSC design is the obvious possibility to use two sensitizers with complementary spectral response, one on each type of semiconductor.

The second advantage of such a design is the expected increase of the open circuit voltage. Indeed, in an n-type DSC, the maximum V_{oc} value is considered to be the energy difference between the oxidation potential of the redox mediator and the energy level of the quasi-Fermi level in the n-type semiconductor. As it is usually TiO_2, we name it $V_{oc}(TiO_2)$. In a p-type DSC, the maximum V_{oc} value is the energy difference between the oxidation potential of the redox mediator and the energy level of the quasi-Fermi level of the free electrons in the p-type semiconductor. In the case of NiO, we name it $V_{oc}(NiO)$. In the tandem DSC, the maximum value for the open circuit voltage is the sum of both components, $V_{oc} = V_{oc}(TiO_2) + V_{oc}(NiO)$. The proof of concept of this strategy has been reported in 2000, using N719 as sensitizer for the photoanode and erythrosine B as sensitizer for the photocathode.[120] The performances of this system has been improved by more than 50% (from $\eta = 0.39\%$ to 0.66% under AM 1.5) by using a mesoporous NiO film of higher quality.[121]

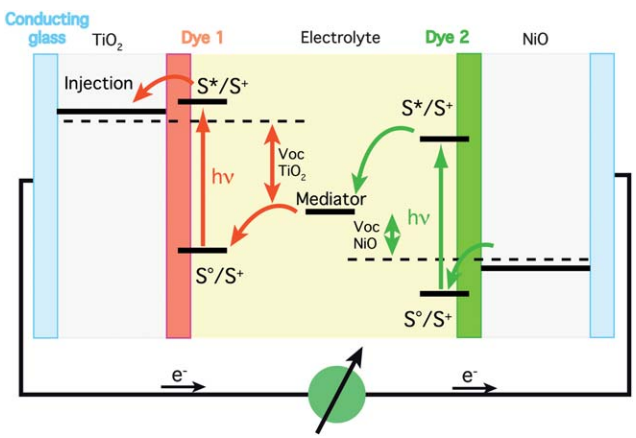

Fig. 27 Operating principles of tandem dye-sensitized solar cell composed of n- and p-type semiconductor.

Due to the definition of V_{oc} in a tandem DSC, it can be deduced that the electrochemical potential of the redox mediator has no impact on its value. Therefore it is possible to replace the I^-/I_3^- couple by the $Co^{II/III}$(4,4′-di-*tert*-butyl-2,2′-dipyridyl)$_3$ in the electrolyte without impacting the V_{oc}.[122] Finally, using a dye having a variable-length oligothiophene bridge, a tandem DSC with a power conversion efficiency of 2.42% was obtained.[123] The use of the tailored bridges length allowed for the control over the recombination events. Taking into account that in this case, the spectral responses of both dyes were similar, this is a very promising result for future devices using dyes with a complementary spectral response.

Summary and outlook

We have given an overview of panchromatic engineering strategies for dye-sensitized solar cells: panchromatic single sensitizers, co-sensitization, energy down conversion (relay dye), and tandem configuration. For the single dyes, we briefly reviewed the Ru(II) complexes, an organic dye, and PbS as a sensitizer showing very broad light harvesting characteristics. The photocurrent onset is around 900 nm but the IPCE in the longer wavelength range is still low because of the low extinction coefficient. Hence, judicious molecular engineering of the dye structure will allow for further increasing the light harvesting in the 700–900 nm region. In this respect ruthenium complexes of quaterpyridyl derivatives[124] and Os(II) complex[36,125] have great potential. A nearly vertical rise of the photocurrent close to the 920 nm absorption threshold would increase the short circuit photocurrent from currently 20.5 to about 28 mA cm^{-2} raising the overall efficiency to about 15% assuming the other parameters, V_{oc} and ff are maintained. In this respect, an unprecedented high photocurrent, 26.6 mA cm^{-2} with a confidential dye has recently been shown by Segawa in the 5th Aseanian conference on dye-sensitized and organic solar cell.[126] This result shows a great promise in terms of the light harvesting even though it is needed to increase a low V_{oc}, 450 mV.

It remains a challenge to design a single sensitizer that is able to absorb efficiently over the entire spectrum from 400 to 920 nm that fulfills all the requirements for obtaining an efficient device. In this respect, the combination of multiple dyes appears to be a promising approach to obtain panchromatic systems. Organic dyes could be advantageous for this application due to their extremely high molar extinction coefficients. However, the limited number of adsorption sites on the TiO_2 surface for dye molecules and unfavorable interactions among dye molecules place a constraint on the light absorption achievable by co-sensitization. In this respect, a promising combination for co-sensitization has been developed, incorporating an organic dye

with the N749 dye. The organic dye does not compete with the N749 dye to stain the TiO_2 surface and in addition increases the IPCE of N749. Selective dye adsorption methods have also been developed to avoid the limitation of co-sensitization. But, further optimization is needed to fully exploit the performance increase, since the efficiencies obtained so far do not eclipse the champion performance obtained by single dye. We also demonstrated a new DSC architecture where highly luminescent energy relay dyes (ERDs) dissolved inside the electrolyte absorb higher energy photons and transfer their energy to the sensitizing dye *via* Förster resonance energy transfer (FRET). Since the attached dye only has to absorb light over a smaller spectral region, it can be chosen to have a stronger and narrower absorption spectrum. Additionally, the dye can be red-shifted to absorb near-IR since the energy relay dye performs the task of adsorbing higher energy photons. Furthermore, it is possible to place multiple ERDs with complementary absorption spectra to tailor light absorption inside the device. In summary, the addition of energy relay dyes into the electrolyte makes the overall absorption spectrum wider and stronger for the same film thickness. The average excitation transfer energy seems to be strongly governed by competitive quenching by an electrolyte. The best combination so far showed over 95% of the average excitation transfer energy. In order to achieve a further increase in IPCE, a high light absorbing efficiency of the energy relay dye is essential. Hence, the energy relay dye should be designed to be soluble in and not greatly quenched by the electrolyte media as well as being designed to have a high molar extinction coefficient. Not only that, a wider spectral response in the system is needed to design to accomplish further performance enhancement.

Ideally, fractions of the solar spectrum are absorbed by different solar cells stacked on top of each other. We have shown that a monolithic DSC/CIGS tandem device has the potential for increased efficiency over a mechanically stacked device due to increased light transmission to the bottom cell and demonstrated a monolithic DSC/CIGS device with an initial efficiency of 12.2%. We expect to make full use of the optical advantages of this setup and to surpass the 15.1% efficiency benchmark given by the stacked device with a suitable protective intermediate layer inhibiting the degradation mechanism at the electrolyte/CIGS interface. In a p-type DSC, the photoexcited sensitizer is reductively quenched by hole injection into the quasi-Fermi level of a p-type semiconductor. Combination with an n-type DSC is promising because of advantages, complementary spectral response and high V_{oc} value. But a conversion efficiency is not fully exploited. In this respect, basic research and new material development in this area will be intimately connected with the progress on single semiconductor p-DSC and tandem with n-type DSC.

The nanocrystalline morphology of the oxide semiconductor film is essential for the efficient operation of the DSC. The introduction of optical elements, *i.e.* layers composed of large particles[127–130] or voids,[131–133] or photonic crystal[134–140] will further enhance the device performance. Record-holding DSCs are based on Ru(II) complexes having maximum quantum efficiencies in the range of 500–600 nm. Clearly, enhanced so far, a light harvesting in the red and near-IR is still essential to improve the overall power conversion efficiency. Ito *et al.* have shown an incorporated scattering layer to be an essential component to achieve a high power conversion efficiency.[141] Additional application of this effective strategy looking simple but requiring meticulous optimization may antedate a breakthrough of a power conversion efficiency in a device.

Acknowledgements

We gratefully acknowledge Swiss National Science Foundation and Collaborative Large-Scale Integrating Project ORION FP7-NMP-LA-2009-229036. J.-H. Yum thanks Mrs Rebecca Hill and Mrs Soo-Jin Moon, EPFL for fruitful discussion.

References

1 *World in Transition—Towards Sustainable Energy Systems, German Advisory Council on Global Change*, 2003, http://www.wbgu.de/wbgu_jg2003_kurz_engl.html.
2 N. Armaroli and V. Balzani, *Angew. Chem., Int. Ed.*, 2007, **46**, 52–66.
3 M. K. Nazeeruddin and M. Grätzel, in *Molecular and Supramolecular Photochemistry*, ed. V. Ramanurthy and K. S. Schanze, Marcel Dekker, New York, 2003, pp. 301–343.
4 M. K. Nazeeruddin, *Special Issue: Michael Graetzel Festschrift, a Tribute for his 60th Birthday: Dye Sensitized Solar Cells*, Elsevier, Amsterdam, 2004.
5 D. Gust, T. A. Moore and A. L. Moore, *Acc. Chem. Res.*, 2009, **42**, 1890–1898.
6 D. G. Nocera, *Inorg. Chem.*, 2009, **48**, 10001–10017.
7 S. Anderson, E. C. Constable, M. P. Dareedwards, J. B. Goodenough, A. Hamnett, K. R. Seddon and R. D. Wright, *Nature*, 1979, **280**, 571–573.
8 M. Grätzel, in *Handbook of Nanostructured Materials and Nanotechnology*, ed. H. S. Nalwa, Academic Press, San Diego, 2000, pp. 527–553.
9 M. Grätzel, *Nature*, 2001, **414**, 338–344.
10 M. A. Green, K. Emery, Y. Hisikawa and W. Warta, *Prog. Photovoltaics*, 2007, **15**, 425–430.
11 M. K. Nazeeruddin and M. Grätzel, in *Encyclopedia of Electrochemistry: Semiconductor Electrodes and Photoelectrochemistry*, ed. A. Bard, M. Startmann and S. Licht, Wieley-VCH, Germany, 2002, pp. 407–431.
12 B. O'Regan and M. Grätzel, *Nature*, 1991, **353**, 737–740.
13 M. Grätzel, *Acc. Chem. Res.*, 2009, **42**, 1788–1798.
14 M. K. Nazeeruddin, S. M. Zakeeruddin, R. Humphry-Baker, M. Jirousek, P. Liska, N. Vlachopoulos, V. Shklover, C. H. Fischer and M. Grätzel, *Inorg. Chem.*, 1999, **38**, 6298–6305.
15 A. Hagfeldt and M. Grätzel, *Acc. Chem. Res.*, 2000, **33**, 269–277.
16 M. Grätzel, *J. Photochem. Photobiol., C*, 2003, **4**, 145–153.
17 M. Grätzel, *Chem. Lett.*, 2005, **34**, 8–13.
18 S. Ardo and G. J. Meyer, *Chem. Soc. Rev.*, 2009, **38**, 115–164.
19 A. Hagfeldt and M. Grätzel, *Chem. Rev.*, 1995, **95**, 49–68.
20 M. K. Nazeeruddin, A. Kay, I. Rodicio, R. Humphrybaker, E. Muller, P. Liska, N. Vlachopoulos and M. Grätzel, *J. Am. Chem. Soc.*, 1993, **115**, 6382–6390.
21 A. F. Haught, *J. Sol. Energy Eng.*, 1984, **106**, 3–15.
22 A. De Vos, in *Endoreversible Thermodynamics of Solar Energy Conversion*, Science Publishers, Oxford, 1992, pp. 301–311.
23 M. K. Nazeeruddin, A. Kay, I. Rodicio, R. Humphrybaker, E. Muller, P. Liska, N. Vlachopoulos and M. Grätzel, *J. Am. Chem. Soc.*, 1993, **115**, 6382–6390.
24 K. Hara, H. Sugihara, Y. Tachibana, A. Islam, M. Yanagida, K. Sayama, H. Arakawa, G. Fujihashi, T. Horiguchi and T. Kinoshita, *Langmuir*, 2001, **17**, 5992–5999.
25 M. Yanagida, T. Yamaguchi, M. Kurashige, K. Hara, R. Katoh, H. Sugihara and H. Arakawa, *Inorg. Chem.*, 2003, **42**, 7921–7931.
26 A. Islam, H. Sugihara and H. Arakawa, *J. Photochem. Photobiol., A*, 2003, **158**, 131–138.
27 M. K. Nazeeruddin and M. Grätzel, in *Structure and Bonding*, ed. D. M. P. Mingos and V. W. W. Yam, 2007, vol. 123, pp. 113–175.
28 M. K. Nazeeruddin, P. Péchy and M. Grätzel, *Chem. Commun.*, 1997, 1705–1706.
29 M. K. Nazeeruddin, P. Péchy, T. Renouard, S. M. Zakeeruddin, R. Humphry-Baker, P. Comte, P. Liska, L. Cevey, E. Costa,

V. Shklover, L. Spiccia, G. B. Deacon, C. A. Bignozzi and M. Grätzel, *J. Am. Chem. Soc.*, 2001, **123**, 1613–1624.
30 M. Grätzel, *J. Photochem. Photobiol., A*, 2004, **168**, 235–235.
31 Y. Chiba, A. Islam, Y. Watanabe, R. Komiya, N. Koide and L. Y. Han, *Jpn. J. Appl. Phys., Part 2*, 2006, **45**, L638–L640.
32 N. Onozawa-Komatsuzaki, M. Yanagida, T. Funaki, K. Kasuga, K. Sayama and H. Sugihara, *Inorg. Chem. Commun.*, 2009, **12**, 1212–1215.
33 A. Islam, F. A. Chowdhury, Y. Chiba, R. Komiya, N. Fuke, N. Ikeda and L. Y. Han, *Chem. Lett.*, 2005, **34**, 344–345.
34 T. Funaki, M. Yanagida, N. Onozawa-Komatsuzaki, K. Kasuga, Y. Kawanishi and H. Sugihara, *Chem. Lett.*, 2009, **38**, 62–63.
35 T. Funaki, M. Yanagida, N. Onozawa-Komatsuzaki, K. Kasuga, Y. Kawanishi, M. Kurashige, K. Sayama and H. Sugihara, *Inorg. Chem. Commun.*, 2009, **12**, 842–845.
36 S. Altobello, R. Argazzi, S. Caramori, C. Contado, S. Da Fre, P. Rubino, C. Chone, G. Larramona and C. A. Bignozzi, *J. Am. Chem. Soc.*, 2005, **127**, 15342–15343.
37 B. S. Chen, K. Chen, Y. H. Hong, W. H. Liu, T. H. Li, C. H. Lai, P. T. Chou, Y. Chi and G. H. Lee, *Chem. Commun.*, 2009, 5844–5846.
38 A. Mishra, M. K. R. Fischer and P. Bäuerle, *Angew. Chem., Int. Ed.*, 2009, **48**, 2474–2499.
39 J.-H. Yum and M. K. Nazeeruddin, in *Dye-sensitized Solar Cells*, ed. K. Kalyanasundaram, EPFL Press, 2010, pp. 83–116.
40 H. Tian, X. Yang, R. Chen, A. Hagfeldt and L. Sun, *Energy Environ. Sci.*, 2009, **2**, 674–677.
41 H. N. Tian, X. C. Yang, R. K. Chen, Y. Z. Pan, L. Li, A. Hagfeldt and L. C. Sun, *Chem. Commun.*, 2007, 3741–3743.
42 W. W. Yu, L. H. Qu, W. Z. Guo and X. G. Peng, *Chem. Mater.*, 2003, **15**, 2854–2860.
43 G. Hodes, *J. Phys. Chem. C*, 2008, **112**, 17778–17787.
44 L. Brus, *J. Phys. Chem.*, 1986, **90**, 2555–2560.
45 A. P. Alivisatos, *Science*, 1996, **271**, 933–937.
46 R. Vogel, K. Pohl and H. Weller, *Chem. Phys. Lett.*, 1990, **174**, 241–246.
47 I. Oja, A. Belaidi, L. Dloczik, M. C. Lux-Steiner and T. Dittrich, *Semicond. Sci. Technol.*, 2006, **21**, 520–526.
48 G. Larramona, C. Chone, A. Jacob, D. Sakakura, B. Delatouche, D. Pere, X. Cieren, M. Nagino and R. Bayon, *Chem. Mater.*, 2006, **18**, 1688–1696.
49 C. Levy-Clement, R. Tena-Zaera, M. A. Ryan, A. Katty and G. Hodes, *Adv. Mater.*, 2005, **17**, 1512–1515.
50 O. Niitsoo, S. K. Sarkar, C. Pejoux, S. Ruhle, D. Cahen and G. Hodes, *J. Photochem. Photobiol., A*, 2006, **181**, 306–313.
51 L. J. Diguna, Q. Shen, J. Kobayashi and T. Toyoda, *Appl. Phys. Lett.*, 2007, **91**, 023116.
52 H.-J. Lee, J.-H. Yum, H. C. Leventis, S. M. Zakeeruddin, S. A. Haque, P. Chen, S. I. Seok, M. Gräzel and M. K. Nazeeruddin, *J. Phys. Chem. C*, 2008, **112**, 11600–11608.
53 K. Ernst, R. Engelhardt, K. Ellmer, C. Kelch, H. J. Muffler, M. C. Lux-Steiner and R. Konenkamp, *Thin Solid Films*, 2001, **387**, 26–28.
54 T. Dittrich, D. Kieven, M. Rusu, A. Belaidi, J. Tornow, K. Schwarzburg and M. Lux-Steiner, *Appl. Phys. Lett.*, 2008, **93**, 053113.
55 M. Page, O. Niitsoo, Y. Itzhaik, D. Cahen and G. Hodes, *Energy Environ. Sci.*, 2009, **2**, 220–223.
56 I. Kaiser, K. Ernst, C. H. Fischer, R. Konenkamp, C. Rost, I. Sieber and M. C. Lux-Steiner, *Sol. Energy Mater. Sol. Cells*, 2001, **67**, 89–96.
57 J. J. Peterson and T. D. Krauss, *Nano Lett.*, 2006, **6**, 510–514.
58 I. Robel, M. Kuno and P. V. Kamat, *J. Am. Chem. Soc.*, 2007, **129**, 4136–4137.
59 B. R. Hyun, Y. W. Zhong, A. C. Bartnik, L. F. Sun, H. D. Abruna, F. W. Wise, J. D. Goodreau, J. R. Matthews, T. M. Leslie and N. F. Borrelli, *Acs Nano*, 2008, **2**, 2206–2212.
60 H.-J. Lee, P. Chen, S.-J. Moon, F. Sauvage, K. Sivula, T. Bessho, D. R. Gamelin, P. Comte, S. M. Zakeeruddin, S. I. Seok, M. Grätzel and M. K. Nazeeruddin, *Langmuir*, 2009, **25**, 7602–7608.
61 W. Zhao, Y. J. Hou, X. S. Wang, B. W. Zhang, Y. Cao, R. Yang, W. B. Wang and X. R. Xiao, *Sol. Energy Mater. Sol. Cells*, 1999, **58**, 173–183.
62 A. Ehret, L. Stuhl and M. T. Spitler, *J. Phys. Chem. B*, 2001, **105**, 9960–9965.
63 M. M. Nicholson, in *Phthalocyanines: Properties and Applications*, ed. C. C. Leznoff and A. B. P. Lever, VCH publishers, Inc., New York, 1993, pp. 71–117.
64 J.-J. Cid, J.-H. Yum, S.-R. Jang, M. K. Nazeeruddin, E. Martinez-Ferrero, E. Palomares, J. Ko, M. Grätzel and T. Torres, *Angew. Chem., Int. Ed.*, 2007, **46**, 8358–8362.
65 S. Kim, J. K. Lee, S. O. Kang, J. Ko, J.-H. Yum, S. Fantacci, F. De Angelis, D. Di Censo, M. K. Nazeeruddin and M. Grätzel, *J. Am. Chem. Soc.*, 2006, **128**, 16701–16707.
66 R. Y. Ogura, S. Nakane, M. Morooka, M. Orihashi, Y. Suzuki and K. Noda, *Appl. Phys. Lett.*, 2009, **94**, 073308.
67 A. Kay and M. Grätzel, *J. Phys. Chem.*, 1993, **97**, 6272–6277.
68 J.-H. Yum, S. R. Jang, P. Walter, T. Geiger, F. Nüesch, S. Kim, J. Ko, M. Grätzel and M. K. Nazeeruddin, *Chem. Commun.*, 2007, 4680–4682.
69 F. Inakazu, Y. Noma, Y. Ogomi and S. Hayase, *Appl. Phys. Lett.*, 2008, **93**, 093304.
70 P. G. Jessop, T. Ikariya and R. Noyori, *Nature*, 1994, **368**, 231–233.
71 Y. Ogomi, S. Sakaguchi, T. Kado, M. Kono, Y. Yamaguchi and S. Hayase, *J. Electrochem. Soc.*, 2006, **153**, A2294–A2297.
72 K. Lee, S. W. Park, M. J. Ko, K. Kim and N. G. Park, *Nat. Mater.*, 2009, **8**, 665–671.
73 Y. Tachibana, J.-E. Moser, M. Grätzel, D. R. Klug and J. R. Durrant, *J. Phys. Chem.*, 1996, **100**, 20056–20062.
74 S. A. Haque, Y. Tachibana, R. L. Willis, J.-E. Moser, M. Grätzel, D. R. Klug and J. R. Durrant, *J. Phys. Chem. B*, 2000, **104**, 538–547.
75 Y. Tachibana, M. K. Nazeeruddin, M. Grätzel, D. R. Klug and J. R. Durrant, *Chem. Phys.*, 2002, **285**, 127–132.
76 S. A. Haque, Y. Tachibana, D. R. Klug and J. R. Durrant, *J. Phys. Chem. B*, 1998, **102**, 1745–1749.
77 B. C. O'Regan, I. Lopez-Duarte, M. V. Martinez-Diaz, A. Forneli, J. Albero, A. Morandeira, E. Palomares, T. Torres and J. R. Durrant, *J. Am. Chem. Soc.*, 2008, **130**, 2906–2907.
78 B. C. O'Regan, K. Walley, M. Juozapavicius, A. Anderson, F. Matar, T. Ghaddar, S. M. Zakeeruddin, C. Klein and J. R. Durrant, *J. Am. Chem. Soc.*, 2009, **131**, 3541–3548.
79 J. N. Clifford, E. Palomares, M. K. Nazeeruddin, M. Grätzel and J. R. Durrant, *J. Phys. Chem. C*, 2007, **111**, 6561–6567.
80 C. Siegers, J. Hohl-Ebinger, B. Zimmerrnann, U. Wurfel, R. Mulhaupt, A. Hinsch and R. Haag, *ChemPhysChem*, 2007, **8**, 1548–1556.
81 C. Siegers, B. Olah, U. Wurfel, J. Hohl-Ebinger, A. Hinsch and R. Haag, *Sol. Energy Mater. Sol. Cells*, 2009, **93**, 552–563.
82 B. E. Hardin, E. T. Hoke, P. B. Armstrong, J.-H. Yum, T. Torres, J. M. J. Fréchet, M. K. Nazeeruddin, M. Grätzel and M. D. Mcgehee, *Nat. Photonics*, 2009, **3**, 406–411.
83 J.-H. Yum, B. E. Hardin, S. J. Moon, E. Baranoff, F. Nüesch, M. D. McGehee, M. Grätzel and M. K. Nazeeruddin, *Angew. Chem., Int. Ed.*, 2009, **48**, 9277–9280.
84 J.-H. Yum, E. Baranoff, B. E. Hardin, E. T. Hoke, M. D. McGehee, F. Nüesch, M. Grätzel and M. K. Nazeeruddin, *Energy Environ. Sci.*, 2010, **3**, 434–437.
85 X. C. Hu and K. Schulten, *Phys. Today*, 1997, **50**, 28–34.
86 T. Pullerits and V. Sundstrom, *Acc. Chem. Res.*, 1996, **29**, 381–389.
87 X. C. Hu, A. Damjanovic, T. Ritz and K. Schulten, *Proc. Natl. Acad. Sci. U. S. A.*, 1998, **95**, 5935–5941.
88 T. Förster, *Ann. Phys. (Berlin)*, 1948, **2**, 55–75.
89 S. R. Scully, P. B. Armstrong, C. Edder, J. M. J. Frechet and M. D. McGehee, *Adv. Mater.*, 2007, **19**, 2961–2966.
90 J.-H. Yum, P. Walter, S. Huber, D. Rentsch, T. Geiger, F. Nüesch, F. De Angelis, M. Grätzel and M. K. Nazeeruddin, *J. Am. Chem. Soc.*, 2007, **129**, 10320–10321.
91 A. Juris, V. Balzani, F. Barigelletti, S. Campagna, P. Belser and A. Vonzelewsky, *Coord. Chem. Rev.*, 1988, **84**, 85–277.
92 J. R. Lakowicz, *Principles of Fluorescence Spectroscopy*, Plenum Press, New York, 1999.
93 Z. B. Hill, D. B. Rodovsky, J. M. Leger and G. P. Bartholomew, *Chem. Commun.*, 2008, 6594–6596.
94 F. Wurthner, *Chem. Commun.*, 2004, 1564–1579.
95 P. R. Hammond, *Opt. Commun.*, 1979, **29**, 331–333.
96 B. E. Hardin, J.-H. Yum, E. T. Hoke, Y. C. Jun, P. Péchy, T. Torres, M. L. Brongersma, M. K. Nazeeruddin, M. Grätzel and M. D. McGehee, *Nano Lett.*, 2010, **10**, 3077–3083.

97 G. K. Mor, J. Basham, M. Paulose, S. Kim, O. K. Varghese, A. Vaish, S. Yoriya and C. A. Grimes, *Nano Lett.*, 2010, **10**, 2387–2394.
98 W. Shockley and H. J. Queisser, *J. Appl. Phys.*, 1961, **32**, 510–519.
99 S. P. Bremner, M. Y. Levy and C. B. Honsberg, *Prog. Photovoltaics*, 2008, **16**, 225–233.
100 C. H. Henry, *J. Appl. Phys.*, 1980, **51**, 4494–4500.
101 A. Marti and G. L. Araujo, *Sol. Energy Mater. Sol. Cells*, 1996, **43**, 203–222.
102 M. Murayama and T. Mori, *J. Phys. D: Appl. Phys.*, 2007, **40**, 1664–1668.
103 J. Usagawa, S. S. Pandey, S. Hayase, M. Kono and Y. Yamaguchi, *Appl. Phys. Express*, 2009, **2**, 062203.
104 T. Yamaguchi, Y. Uchida, S. Agatsuma and H. Arakawa, *Sol. Energy Mater. Sol. Cells*, 2009, **93**, 733–736.
105 M. K. Nazeeruddin, F. De Angelis, S. Fantacci, A. Selloni, G. Viscardi, P. Liska, S. Ito, T. Bessho and M. Grätzel, *J. Am. Chem. Soc.*, 2005, **127**, 16835–16847.
106 F. Gao, Y. Wang, D. Shi, J. Zhang, M. K. Wang, X. Y. Jing, R. Humphry-Baker, P. Wang, S. M. Zakeeruddin and M. Grätzel, *J. Am. Chem. Soc.*, 2008, **130**, 10720–10728.
107 Y. M. Cao, Y. Bai, Q. J. Yu, Y. M. Cheng, S. Liu, D. Shi, F. F. Gao and P. Wang, *J. Phys. Chem. C*, 2009, **113**, 6290–6297.
108 C. Y. Chen, M. K. Wang, J. Y. Li, N. Pootrakulchote, L. Alibabaei, C. H. Ngoc-le, J. D. Decoppet, J. H. Tsai, C. Grätzel, C. G. Wu, S. M. Zakeeruddin and M. Grätzel, *Acs Nano*, 2009, **3**, 3103–3109.
109 R. W. Birkmire and E. Eser, *Annu. Rev. Mater. Sci.*, 1997, **27**, 625–653.
110 S. Seyrling, S. Calnan, S. Bucheler, J. Hupkes, S. Wenger, D. Bremaud, H. Zogg and A. N. Tiwari, *Thin Solid Films*, 2009, **517**, 2411–2414.
111 P. Liska, K. R. Thampi, M. Grätzel, D. Bremaud, D. Rudmann, H. M. Upadhyaya and A. N. Tiwari, *Appl. Phys. Lett.*, 2006, **88**, 203103.
112 S. Wenger, S. Seyrling, A. N. Tiwari and M. Grätzel, *Appl. Phys. Lett.*, 2009, **94**, 173508.
113 K. Yamamoto, A. Nakajima, M. Yoshimi, T. Sawada, S. Fukuda, T. Suezaki, M. Ichikawa, Y. Koi, M. Goto, T. Meguro, T. Matsuda, M. Kondo, T. Sasaki and Y. Tawada, *Prog. Photovoltaics*, 2005, **13**, 489–494.
114 J. Y. Kim, K. Lee, N. E. Coates, D. Moses, T. Q. Nguyen, M. Dante and A. J. Heeger, *Science*, 2007, **317**, 222–225.
115 R. R. King, D. C. Law, K. M. Edmondson, C. M. Fetzer, G. S. Kinsey, H. Yoon, R. A. Sherif and N. H. Karam, *Appl. Phys. Lett.*, 2007, **90**, 183516.
116 S. Seyrling, S. Bücheler, A. Chirila, J. Perrenoud, S. Wenger, T. Nakada, M. Grätzel and A. N. Tiwari, in *The 34th IEEE Photovoltaic Specialists Conference (PVSC)*, Philadelphia, 2009, pp. 622–625.
117 S. Wenger, *Ecole Polytechnique Fédérale de Lausanne*, 2010.
118 J. He, H. Lindstrom, A. Hagfeldt and S. E. Lindquist, *J. Phys. Chem. B*, 1999, **103**, 8940–8943.
119 F. Odobel, L. Le Pleux, Y. Pellegrin and E. Blart, *Acc. Chem. Res.*, 2010, **43**, 1063–1071.
120 J. He, H. Lindström, A. Hagfeldt and S.-E. Lindquist, *Sol. Energy Mater. Sol. Cells*, 2000, **62**, 265–273.
121 A. Nakasa, E. Suzuki, H. Usami and H. Fujimatsu, *Chem. Lett.*, 2005, **34**, 428–429.
122 E. A. Gibson, A. L. Smeigh, L. Le Pleux, J. Fortage, G. Boschloo, E. Blart, Y. Pellegrin, F. Odobel, A. Hagfeldt and L. Hammarstrom, *Angew. Chem., Int. Ed.*, 2009, **48**, 4402–4405.
123 A. Nattestad, A. J. Mozer, M. K. R. Fischer, Y. B. Cheng, A. Mishra, P. Bauerle and U. Bach, *Nat. Mater.*, 2010, **9**, 31–35.
124 T. Renouard, R. A. Fallahpour, M. K. Nazeeruddin, R. Humphry-Baker, S. I. Gorelsky, A. B. P. Lever and M. Grätzel, *Inorg. Chem.*, 2002, **41**, 367–378.
125 T. Yamaguchi, T. Miyabe, T. Ono and H. Arakawa, *Chem. Commun.*, 2010, **46**, 5802–5804.
126 H. Segawa, in *The 5th Aseanian Conference on Dye-Sensitized and Organic Solar Cell*, Huangshan, August 25–28, 2010.
127 Z. S. Wang, H. Kawauchi, T. Kashima and H. Arakawa, *Coord. Chem. Rev.*, 2004, **248**, 1381–1389.
128 S. Hore, C. Vetter, R. Kern, H. Smit and A. Hinsch, *Sol. Energy Mater. Sol. Cells*, 2006, **90**, 1176–1188.
129 S. Ito, S. M. Zakeeruddin, R. Humphry-Baker, P. Liska, R. Charvet, P. Comte, M. K. Nazeeruddin, P. Péchy, M. Takata, H. Miura, S. Uchida and M. Grätzel, *Adv. Mater.*, 2006, **18**, 1202–1205.
130 H. J. Koo, J. Park, B. Yoo, K. Yoo, K. Kim and N.-G. Park, *Inorg. Chim. Acta*, 2008, **361**, 677–683.
131 S. Hore, P. Nitz, C. Vetter, C. Prahl, M. Niggemann and R. Kern, *Chem. Commun.*, 2005, 2011–2013.
132 H. J. Koo, Y. J. Kim, Y. H. Lee, W. I. Lee, K. Kim and N.-G. Park, *Adv. Mater.*, 2008, **20**, 195–199.
133 S. C. Yang, D. J. Yang, J. Kim, J. M. Hong, H. G. Kim, I. D. Kim and H. Lee, *Adv. Mater.*, 2008, **20**, 1059–1064.
134 S. Nishimura, N. Abrams, B. A. Lewis, L. I. Halaoui, T. E. Mallouk, K. D. Benkstein, J. van de Lagemaat and A. J. Frank, *J. Am. Chem. Soc.*, 2003, **125**, 6306–6310.
135 L. I. Halaoui, N. M. Abrams and T. E. Mallouk, *J. Phys. Chem. B*, 2005, **109**, 6334–6342.
136 A. Mihi and H. Miguez, *J. Phys. Chem. B*, 2005, **109**, 15968–15976.
137 S. H. A. Lee, N. M. Abrams, P. G. Hoertz, G. D. Barber, L. I. Halaoui and T. E. Mallouk, *J. Phys. Chem. B*, 2008, **112**, 14415–14421.
138 S. Colodrero, A. Mihi, L. Haggman, M. Ocana, G. Boschloo, A. Hagfeldt and H. Miguez, *Adv. Mater.*, 2009, **21**, 764–770.
139 L. G. Jin, J. Zhai, L. P. Heng, T. X. Wei, L. P. Wen, L. Jiang, X. X. Zhao and X. Y. Zhang, *J. Photochem. Photobiol., C*, 2009, **10**, 149–158.
140 S. Guldin, S. Huttner, M. Kolle, M. E. Welland, P. Muller-Buschbaum, R. H. Friend, U. Steiner and N. Tetreault, *Nano Lett.*, 2010, **10**, 2303–2309.
141 S. Ito, T. N. Murakami, P. Comte, P. Liska, C. Grätzel, M. K. Nazeeruddin and M. Grätzel, *Thin Solid Films*, 2008, **516**, 4613–4619.